Physics-Based and Data-Driven-Based Algorithms for the Simulation of the Heart Function

Alfio Quarteroni

Politecnico di Milano
and
Ecole Polytechnique Fédérale de Lausanne

July 6, 2023

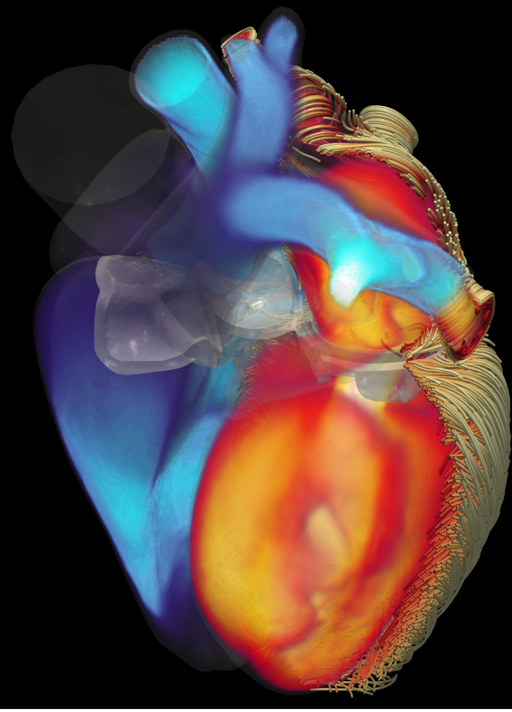

POLITECNICO MILANO 1863

the iHEART simulator

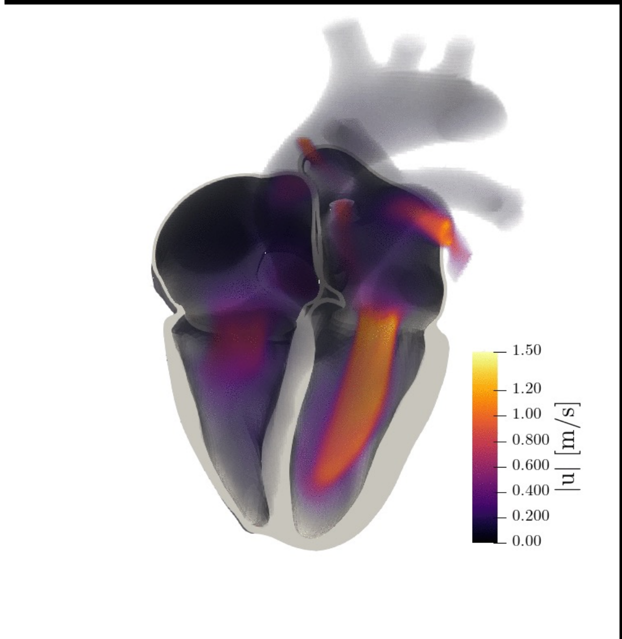

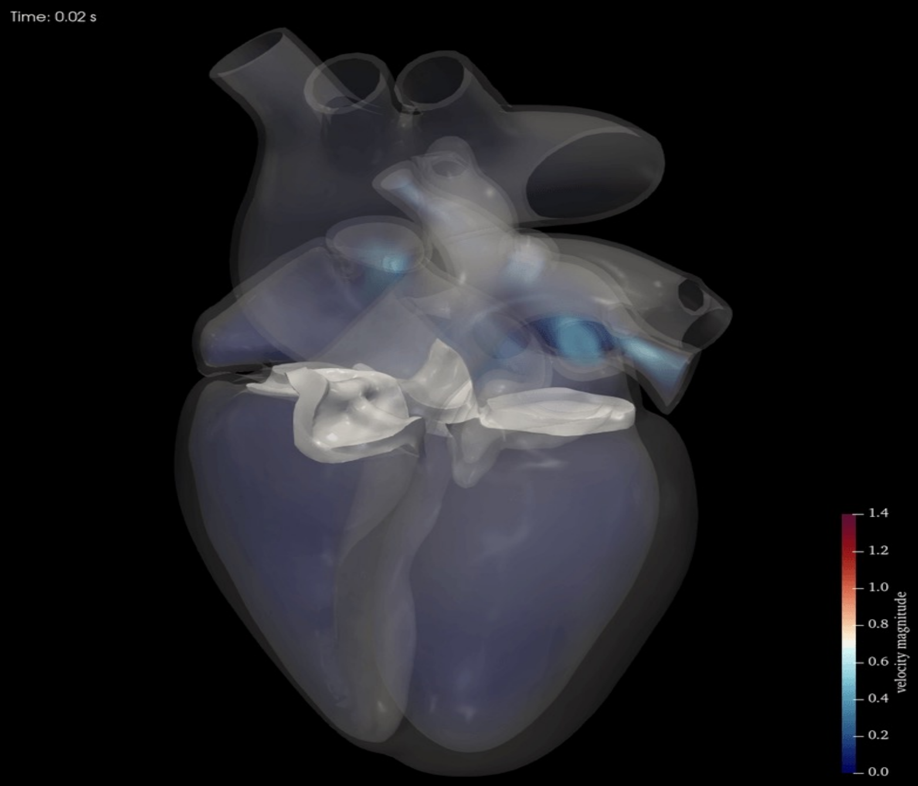

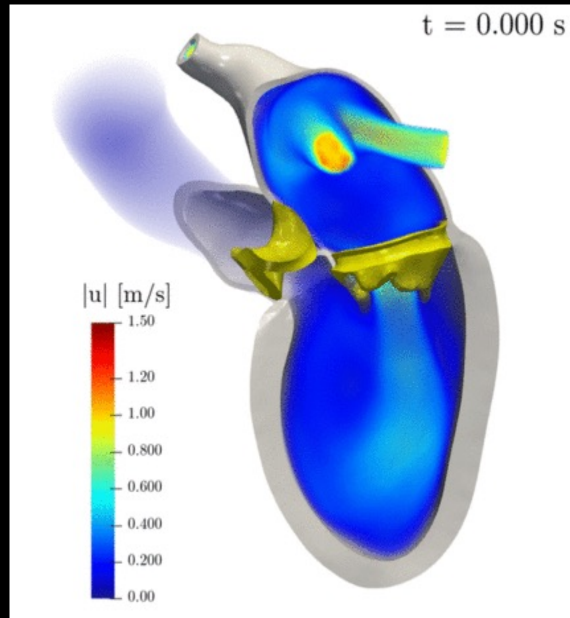

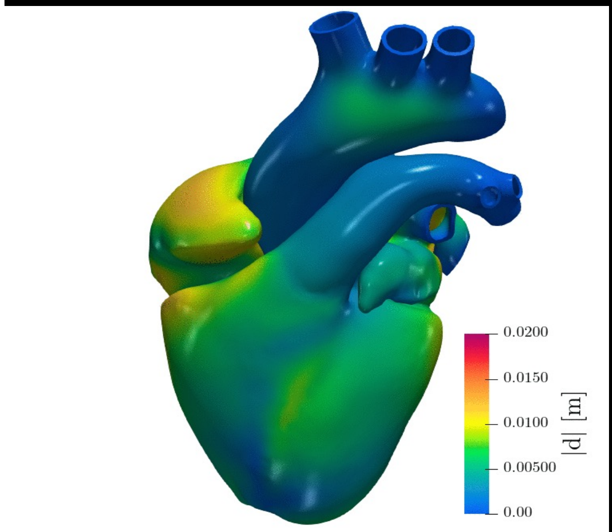

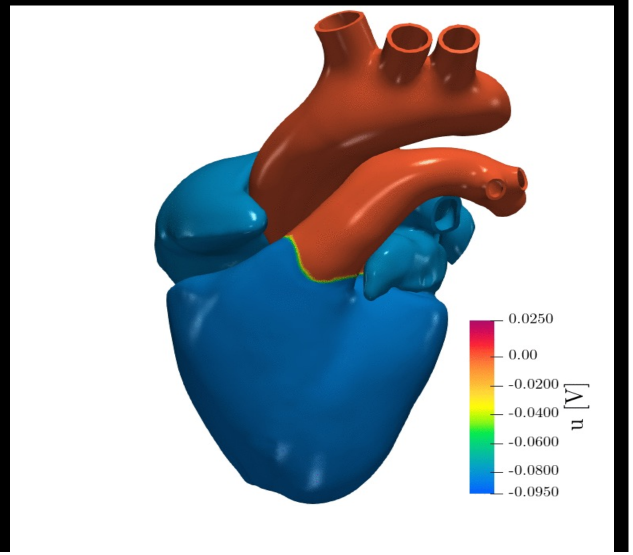

Challenges in modeling the whole heart

Multiphysics and **multiscale** processes

Complex **interaction between each cardiac "physics"**

Complex anatomy, but each cardiac compartment plays a crucial role in the heart function

Different models and parameters in the atria, ventricles, valves, vessels

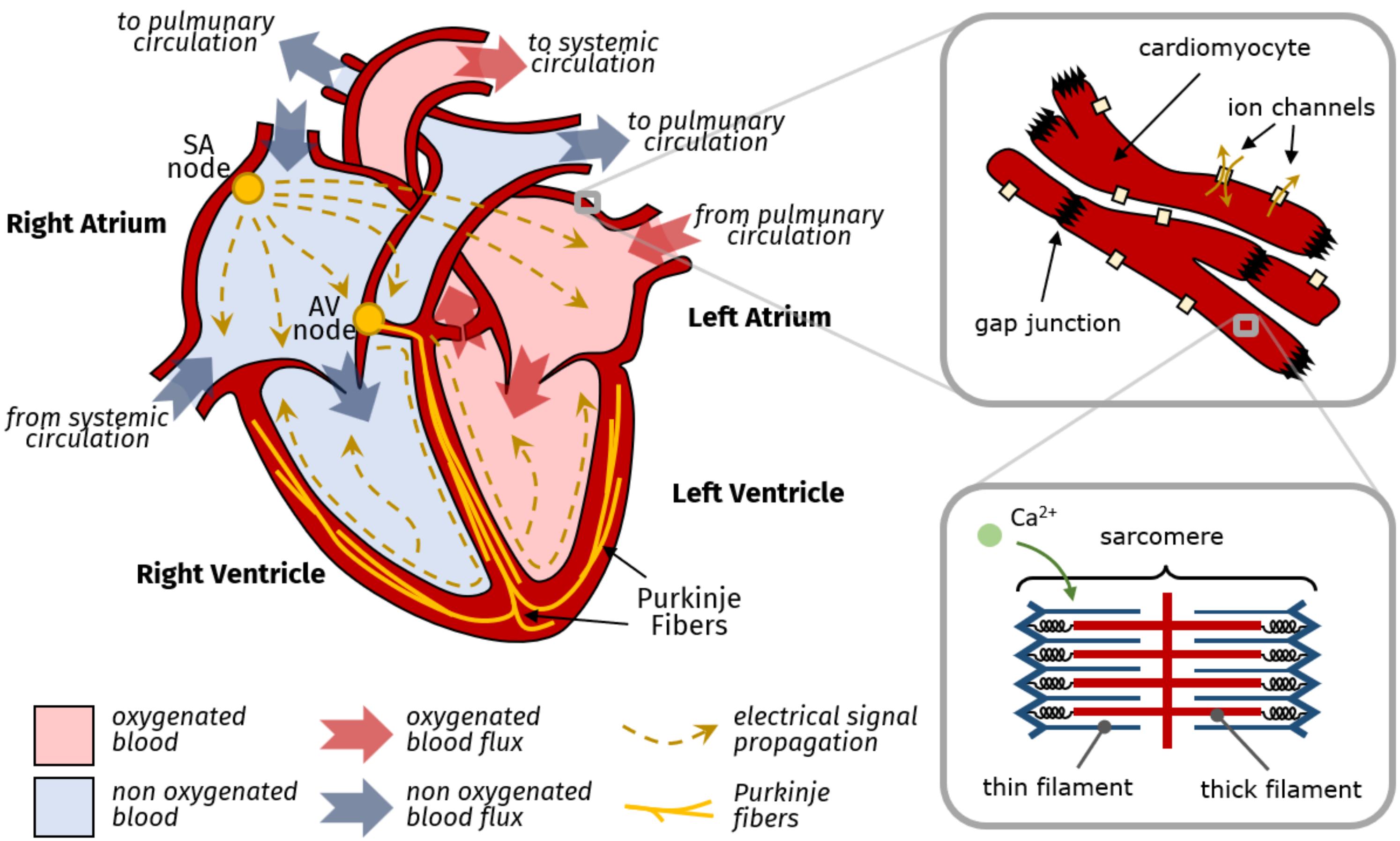

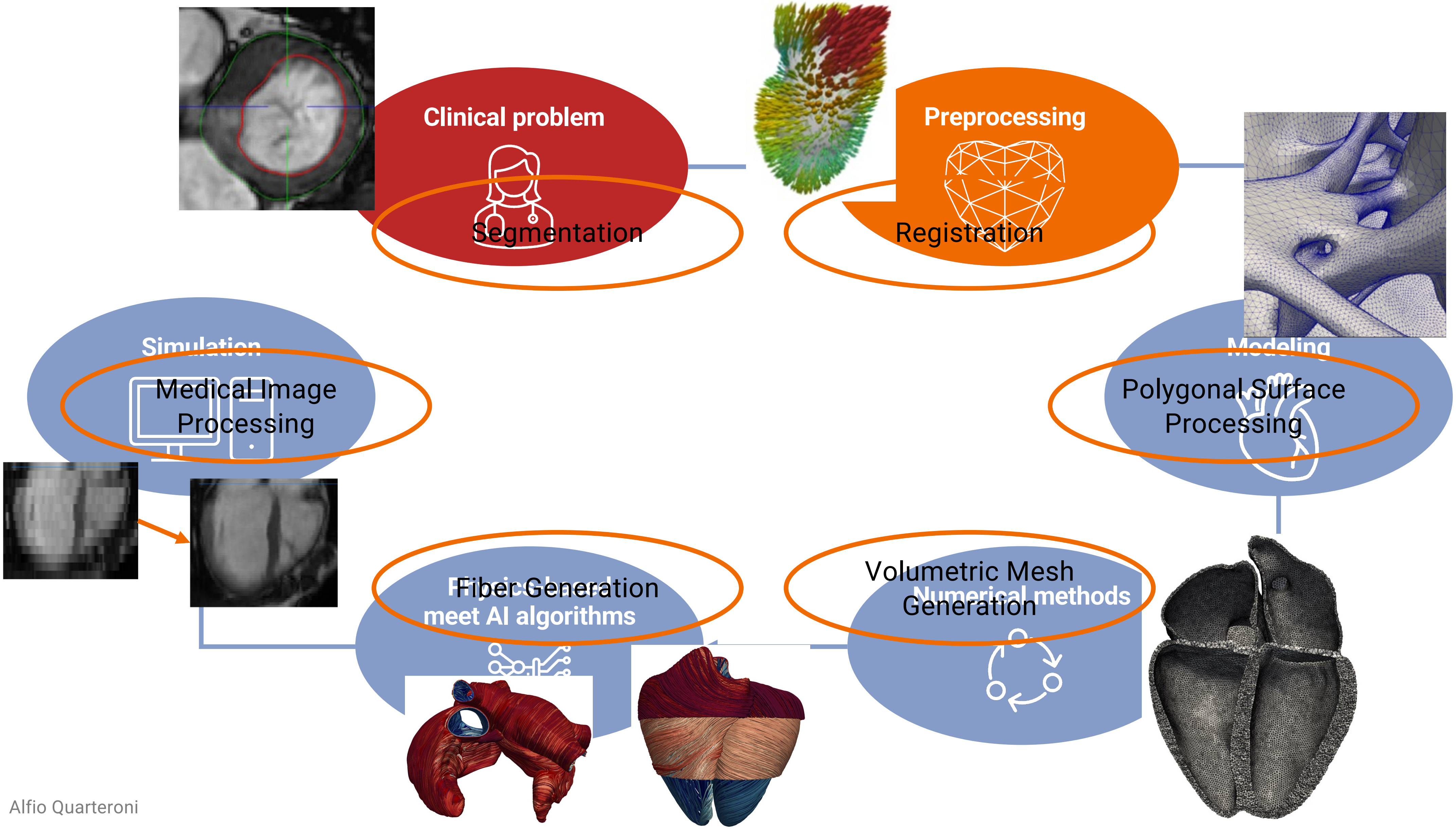

Clinical problem
Segmentation
Preprocessing
Registration
Simulation
Medical Image
Processing
Modeling
Polygonal Surface
Processing
Fiber Generation
meet AI algorithms
Volumetric Mesh
Generation
Numerical methods

Preprocessing

Clinical data and how we use them

CT scans

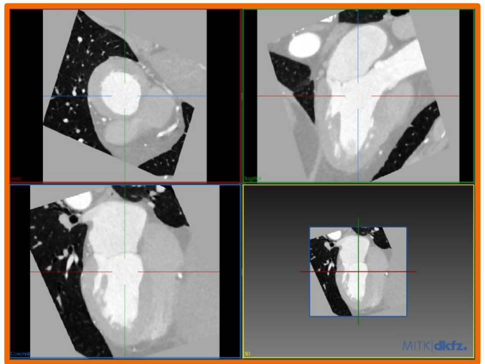

ventricles and coronaries reconstruction

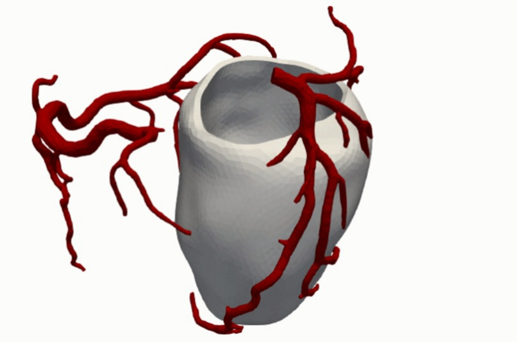

cine MRI

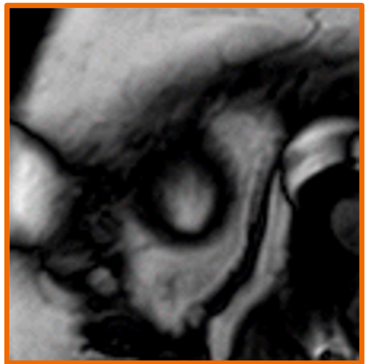

ventricular shape and motion

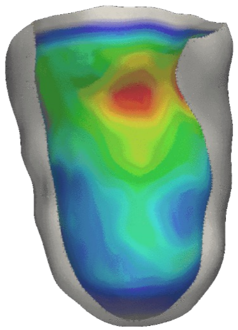

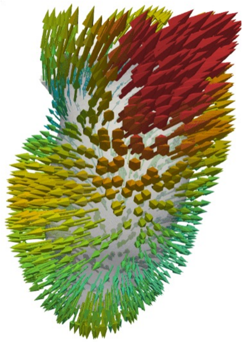

LGE MRI

Late Gadolinium

scar and grey-zone patterns

phase-contrast MRI

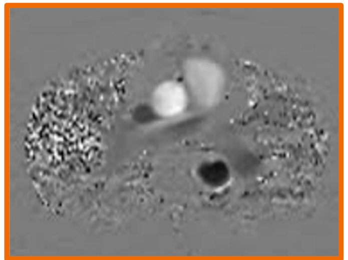

boundary conditions

I. Fumagalli, M. Fedele, C. Vergara, et al., *Computers in Biology and Medicine*, 2020
M. Salvador, M. Fedele, P. Africa, et al., *Computers in Biology and Medicine*, 2021

The Domain Boundaries

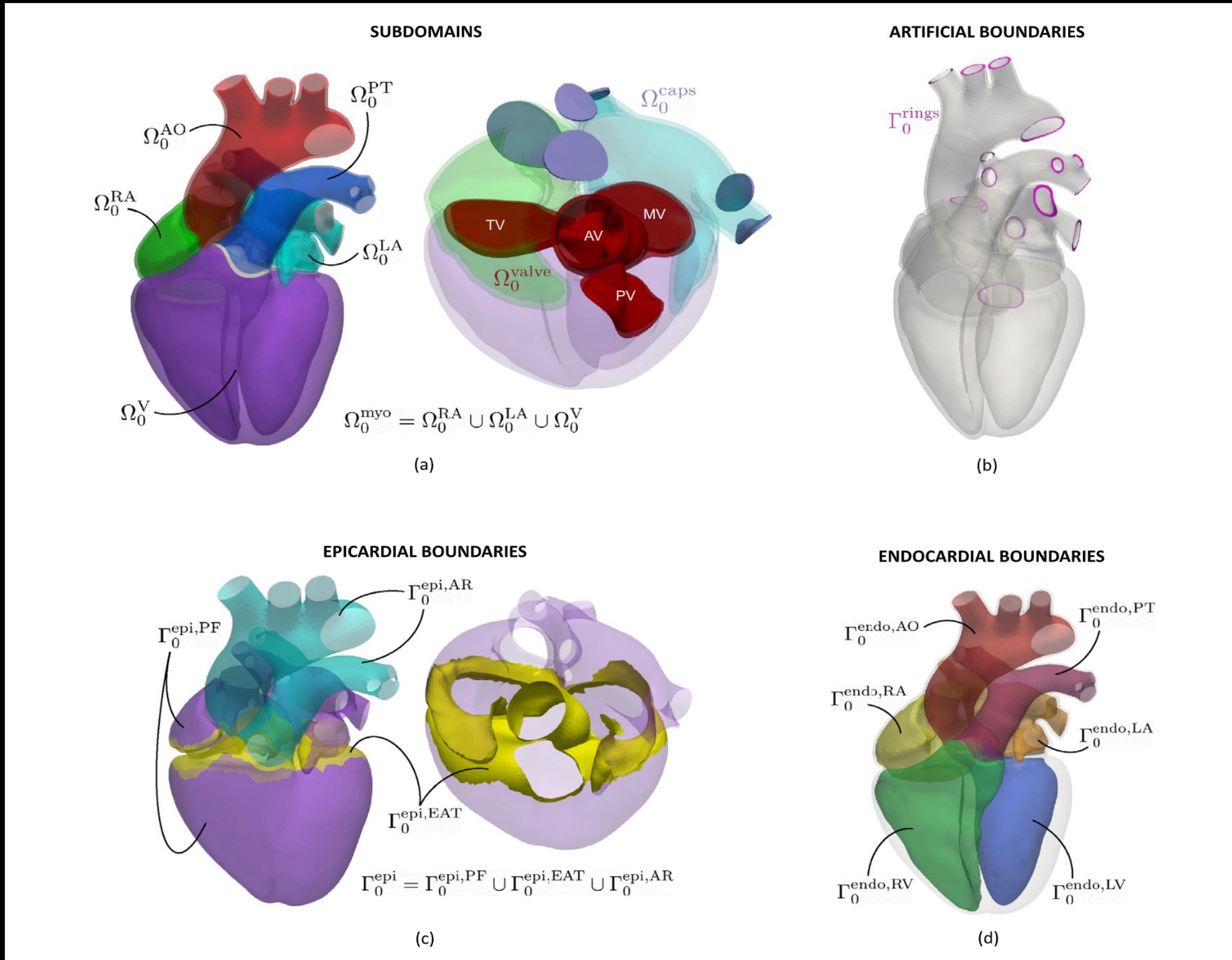

Preprocessing

Generation of cardiac fibers

- fibers are **essential to ensure the cardiac function** (electrophysiology, active and passive mechanics)
- **Laplace-Dirichlet Rule Based** methods (LDRBMs)
- derived from **histological observations** and **DT-MRI data**

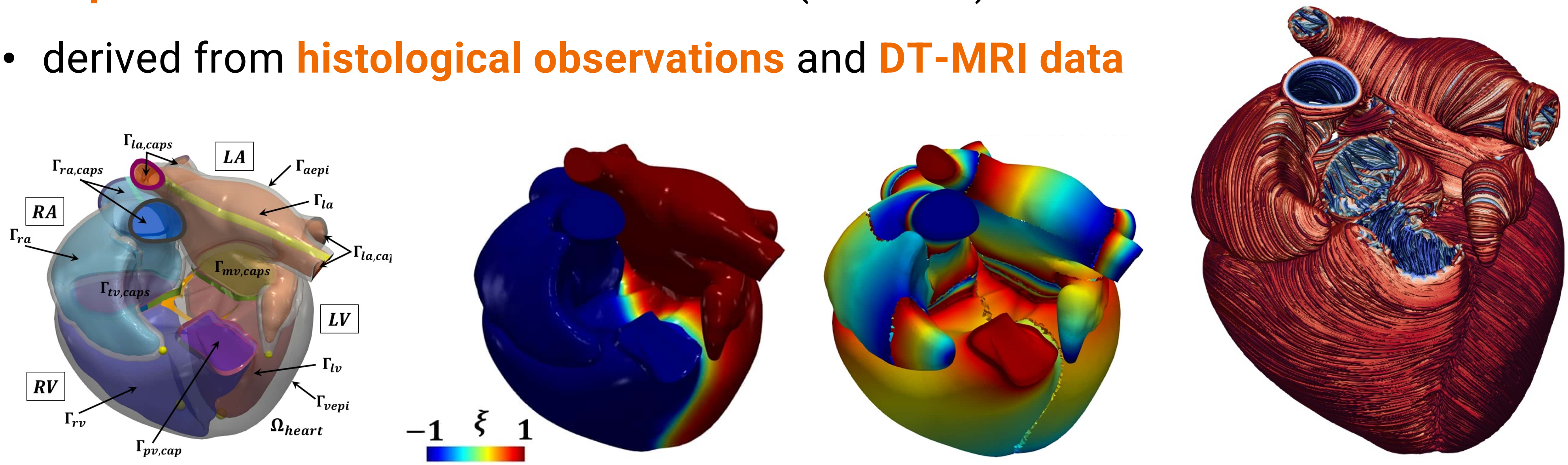

tagged mesh → **scalar potentials** → **Bundles' identification** → **fibers**

R. Piersanti, P. Africa, M. Fedele et al., *Computer Methods in Applied Mechanics and Engineering*, 2021

Transmurality

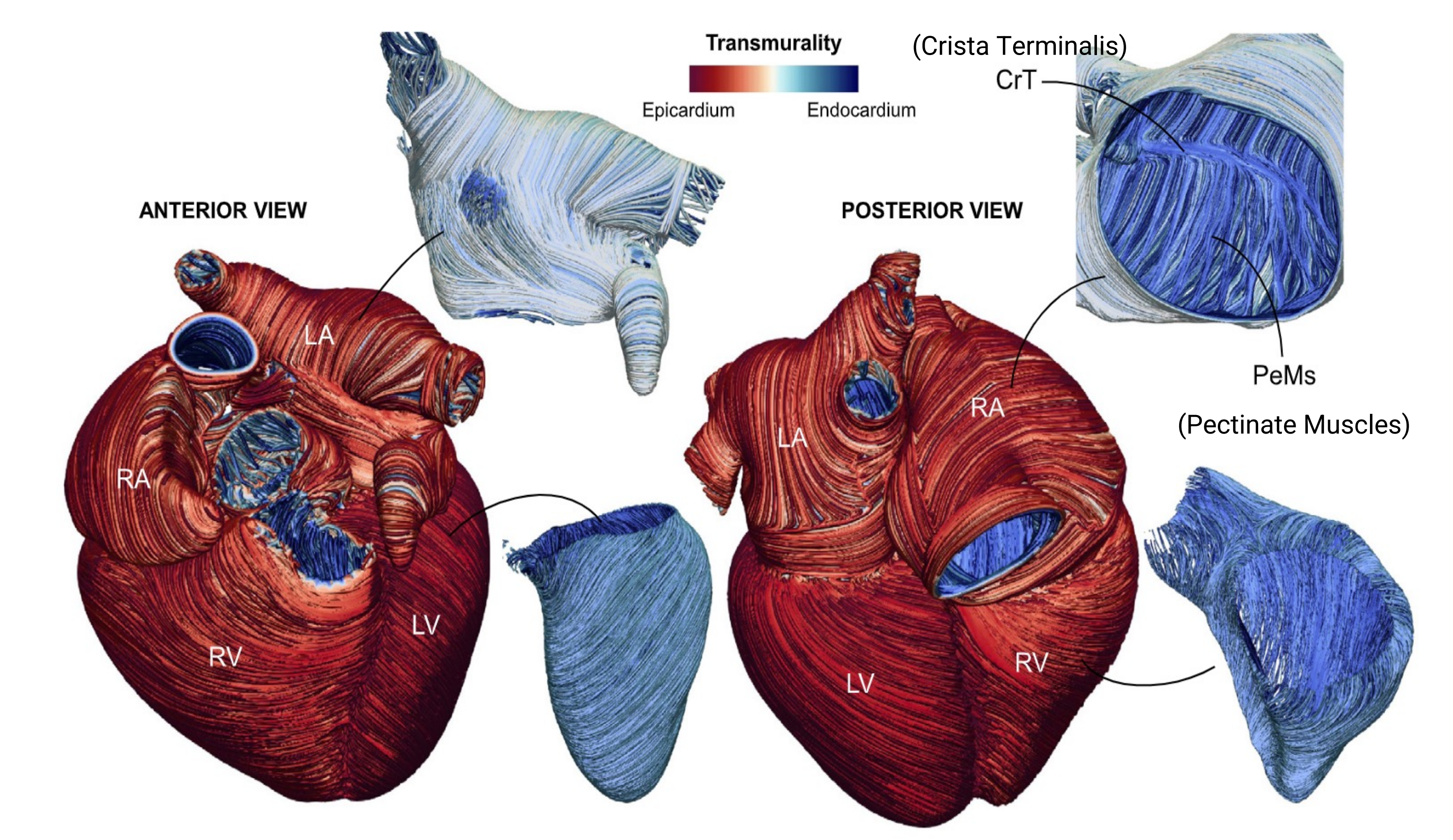

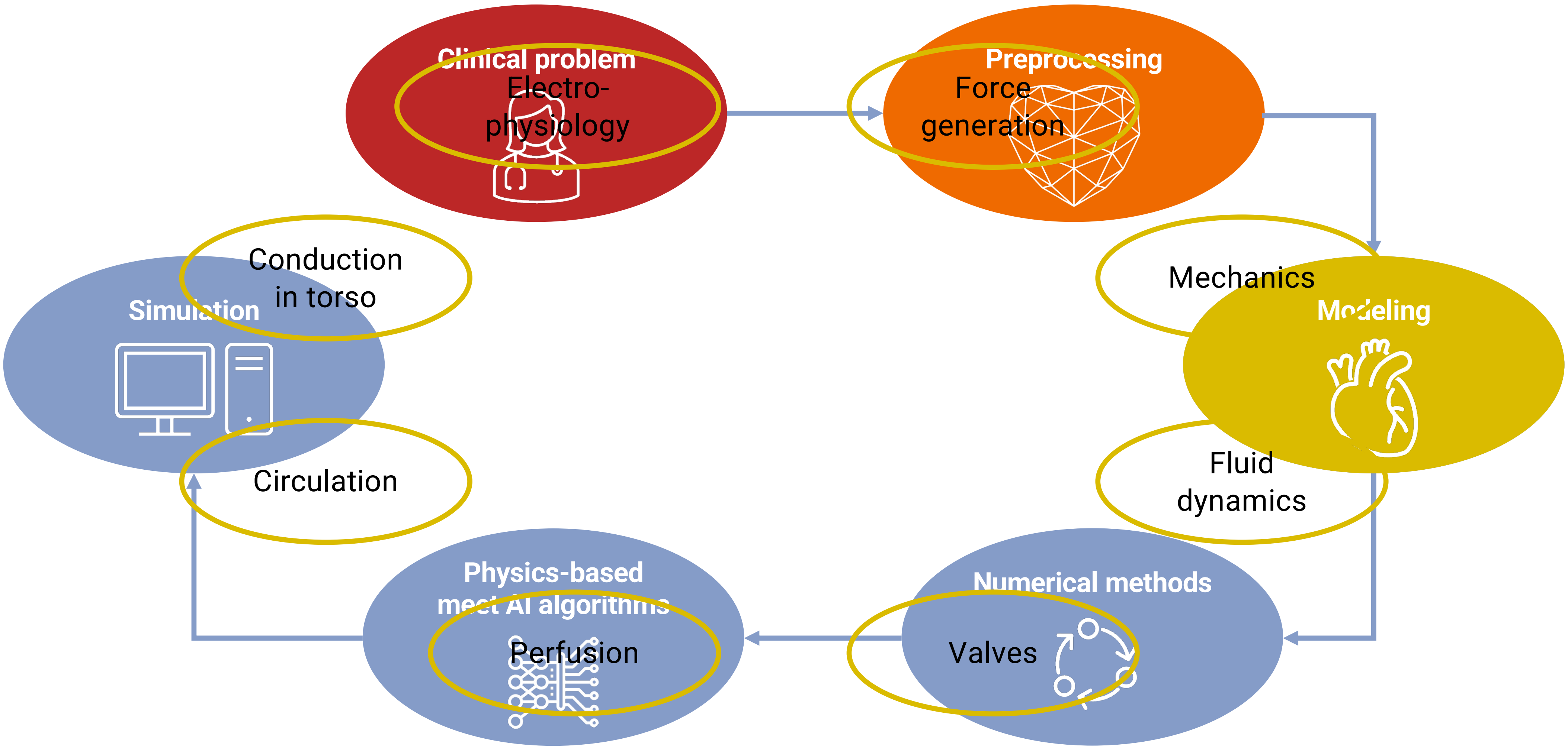
Clinical problem
Electro-
physiology
Preprocessing
Force
generation
Mechanics
Modeling
Fluid
dynamics
Numerical methods
Valves
Physics-based
meet AI algorithms
Perfusion
Simulation
Conduction
in torso
Circulation

The Electromechanics Model

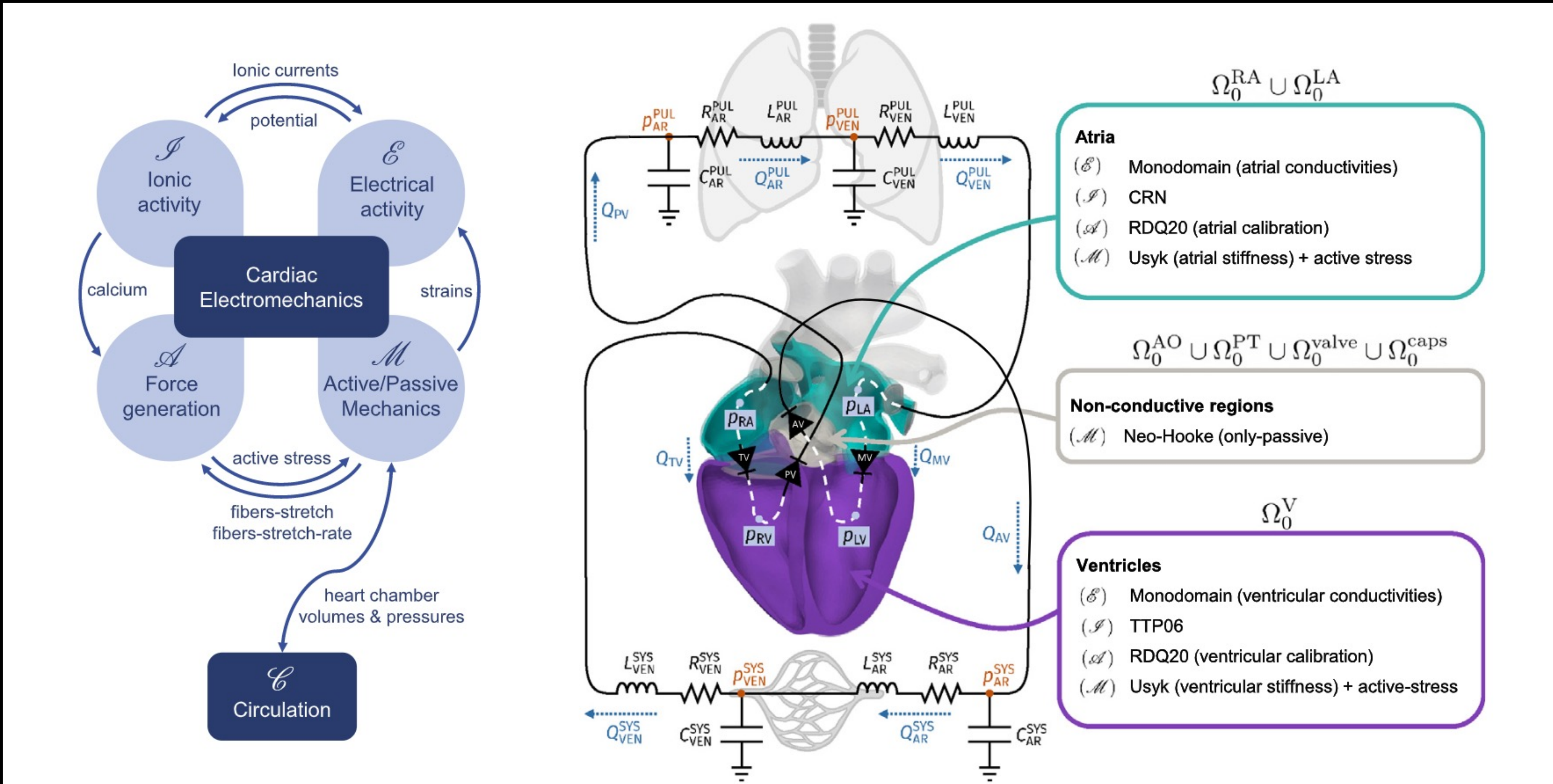

Multiscale modeling in cardiac electro-mechanics

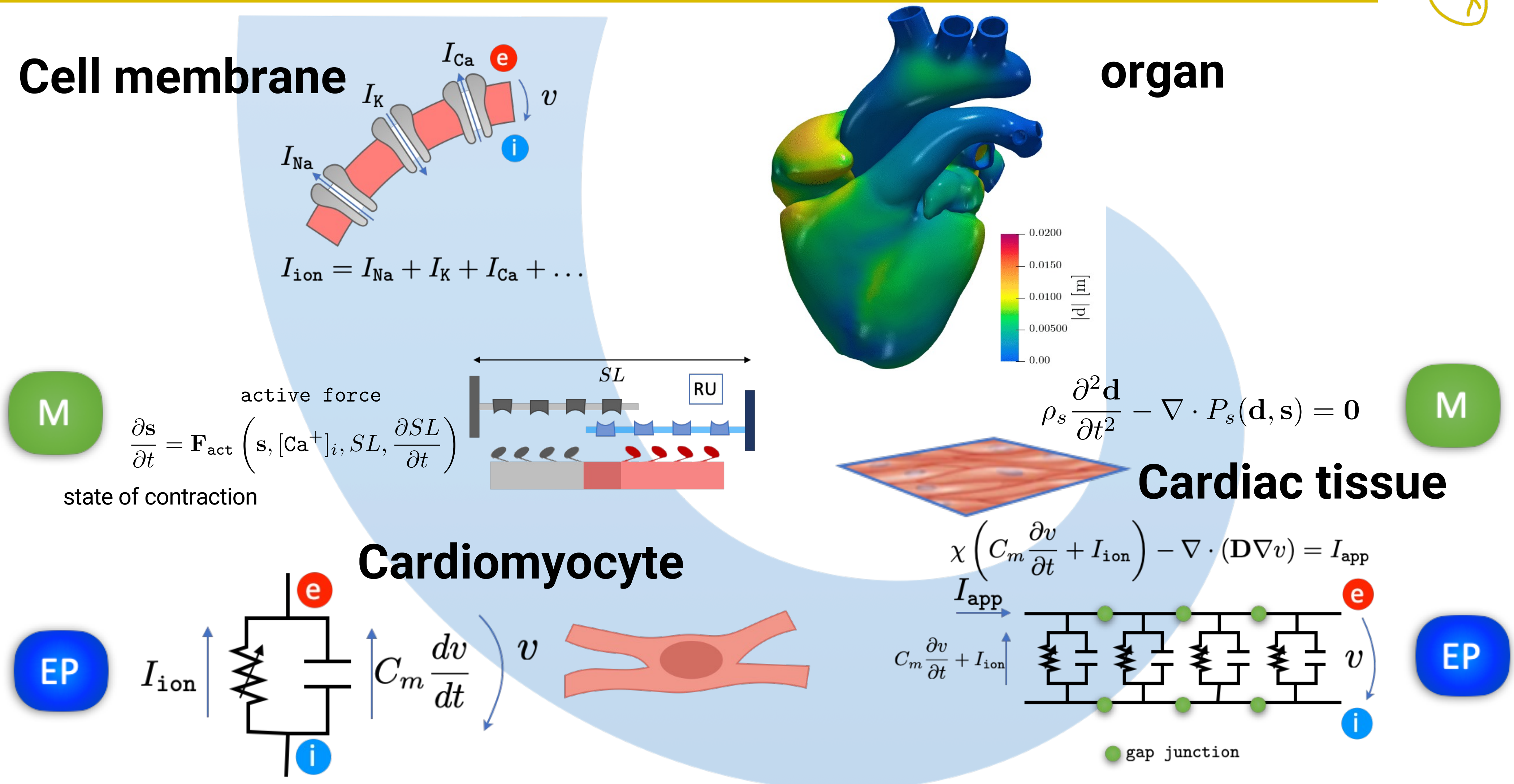

Modeling

The fluid dynamics model

$$\begin{cases} -\nabla \cdot P_{\mathrm{ALE}}(\mathbf{d}_{\mathrm{ALE}}) = \mathbf{0} & \text{in } \widehat{\Omega} \\ \mathbf{d}_{\mathrm{ALE}} = \mathbf{d} & \text{on } \hat{\Sigma} \end{cases} \qquad \mathbf{u}_{\mathrm{ALE}} = \frac{\partial \mathbf{d}_{\mathrm{ALE}}}{\partial t}$$

$$\begin{cases} \rho_{\mathrm{f}} \left[\frac{\partial \mathbf{u}}{\partial t} + ((\mathbf{u} - \mathbf{u}_{\mathrm{ALE}}) \cdot \nabla)\, \mathbf{u} \right] - \nabla \cdot \sigma_{\mathrm{f}}(\mathbf{u}, p) = \mathbf{0} & \text{in } \Omega \\ \nabla \cdot \mathbf{u} = 0 & \text{in } \Omega \end{cases}$$

$$\sigma_{\mathrm{f}}(\mathbf{u}, p) = \mu \left(\nabla \mathbf{u} + \nabla \mathbf{u}^T \right) - pI$$

Unknowns

$\mathbf{d}_{\mathrm{ALE}}$: domain displacement

$\mathbf{u}_{\mathrm{ALE}}$: domain velocity

$\mathbf{u}$: blood velocity

p : blood pressure

- blood modeled as **incompressible, Newtonian**
- **Arbitrary Lagrangian-Eulerian Navier-Stokes**
- **non-linear** domain displacement for robustness
- **VMS-LES** turbulence modeling

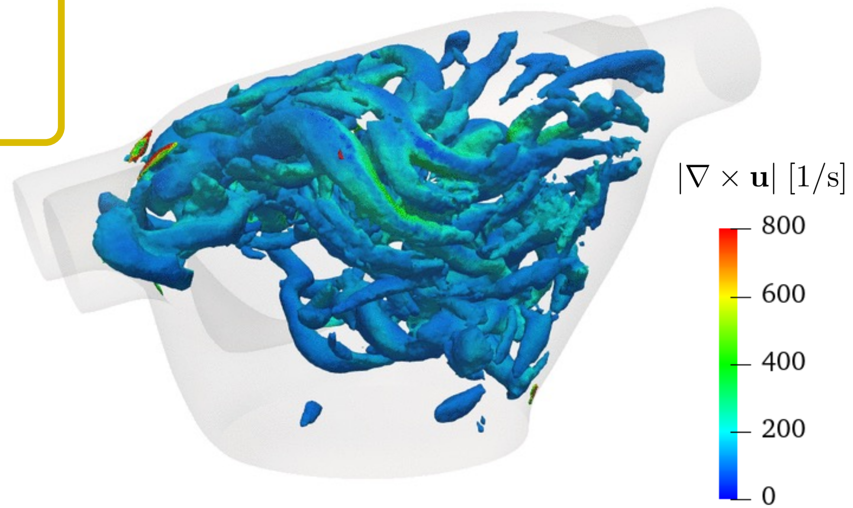

M. Fedele, E. Faggiano, L. Dede', et al., *Biomechanics and Modeling in Mechanobiology*, 2017
A. Zingaro, I. Fumagalli, L. Dede', et al., *Discrete and Continuous Dynamical System – S*, 2022

Resistive Immersed Implicit Surface method for valves

$$\rho_\mathrm{f}\left[\frac{\partial \mathbf{u}}{\partial t} + ((\mathbf{u}-\mathbf{u}_\mathrm{ALE})\cdot\nabla)\,\mathbf{u}\right] - \nabla\cdot\sigma_\mathrm{f}(\mathbf{u},p) + \boldsymbol{\mathcal{R}}(\mathbf{u},\mathbf{u}_\mathrm{ALE}) = \mathbf{0} \qquad \text{in } \Omega$$

$$\boldsymbol{\mathcal{R}}(\mathbf{u},\mathbf{u}_\mathrm{ALE}) = \sum_{\mathrm{k}\in\mathcal{V}} \frac{R_\mathrm{k}}{\varepsilon_\mathrm{k}}\delta_{\varepsilon_\mathrm{k}}\left(\varphi_\mathrm{k}^t(\mathbf{x})\right)(\mathbf{u}-\mathbf{u}_\mathrm{ALE}-\mathbf{u}_{\Gamma_\mathrm{k}})$$

- φ_k^t distance from valve leaflets
- $\delta_{\varepsilon_\mathrm{k}}$ smeared Dirac delta function
- ε_k valve half-thickness
- R_k penalty (resistive) coefficient

Modeling

- valve kinematics defined through $(\varphi_\mathrm{k}^t, \mathbf{u}_{\Gamma_\mathrm{k}})$:
  - pressure jump, or
  - **lumped-parameter valve model**
- **heartbeat phases** and **jets and vortices** induced by the valves correctly captured

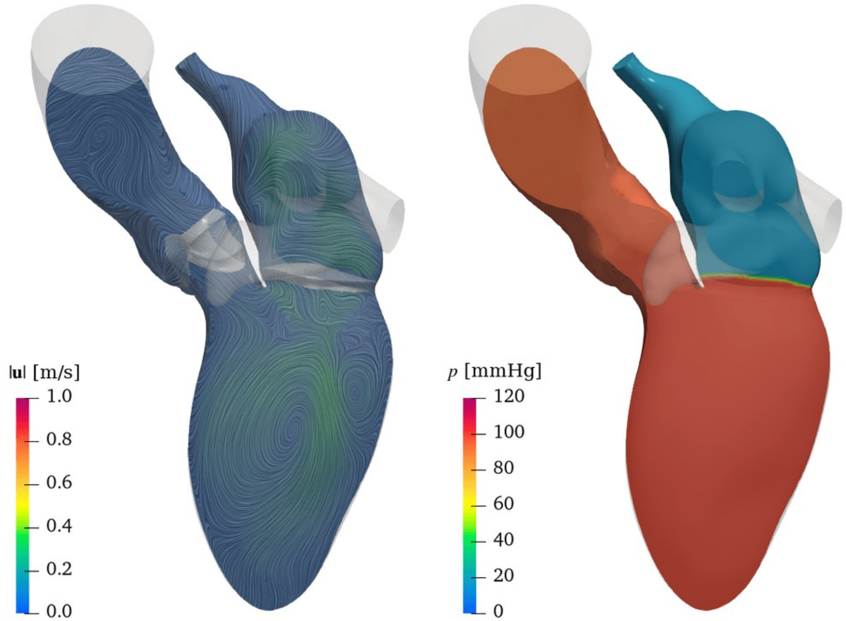

M. Fedele, E. Faggiano, L. Dede', et al., *Biomechanics and Modeling in Mechanobiology*, 2017
A. Zingaro, I. Fumagalli, L. Dede', et al., *Discrete and Continuous Dynamical System – S*, 2022

The Five Atrio-Ventricular Phases

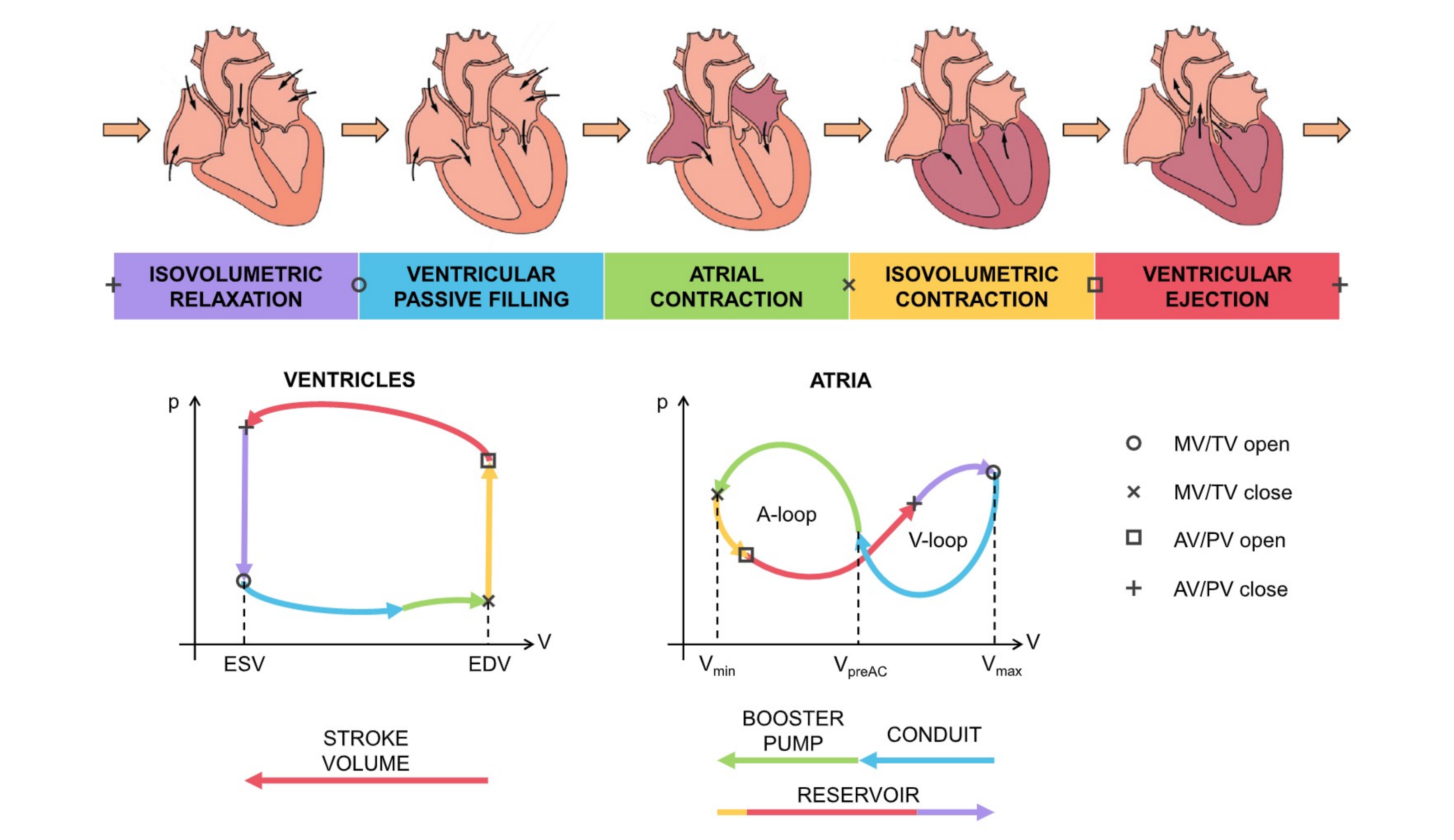

Modeling

The cardiac perfusion model

$$\begin{cases} \mathrm{NS}(\mathbf{u}, p) = \mathbf{0} & \text{in } \Omega_{\mathrm{cor}} \end{cases}$$

Unknowns

$\mathbf{u}$: epicardial cor. velocity

p : epicardial cor. pressure

$\mathbf{u}_{\mathrm{myo}_k}$: *k*-th compartment velocity

p_{myo_k} : *k*-th compartment pressure

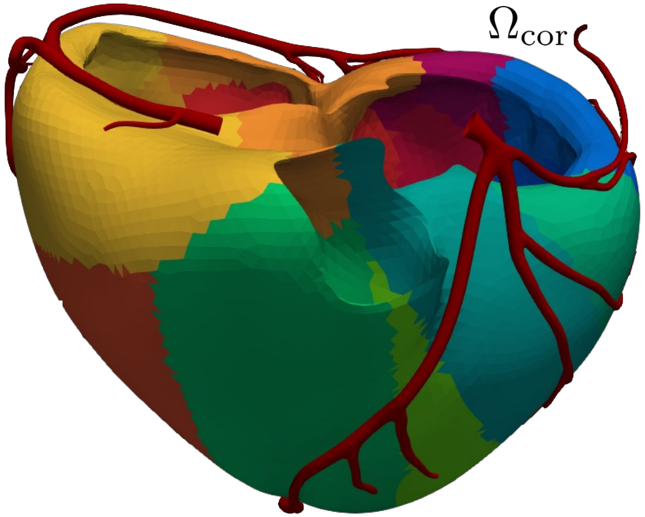

- proximal coronaries: **Navier-Stokes** (NS)
- intramural vessels: **multi-compartment Darcy**
- **two-way coupling** of flow rate and pressure

C. Michler, A.N. Cookson, R. Chabiniok et al., *International Journal of Numerical Methods in Biomedical Engineering*, 2013
S. Di Gregorio, M. Fedele, G. Pontone et al., *Journal of Computational Physics*, 2021

Electromechanics driven CFD-Darcy model for perfusion

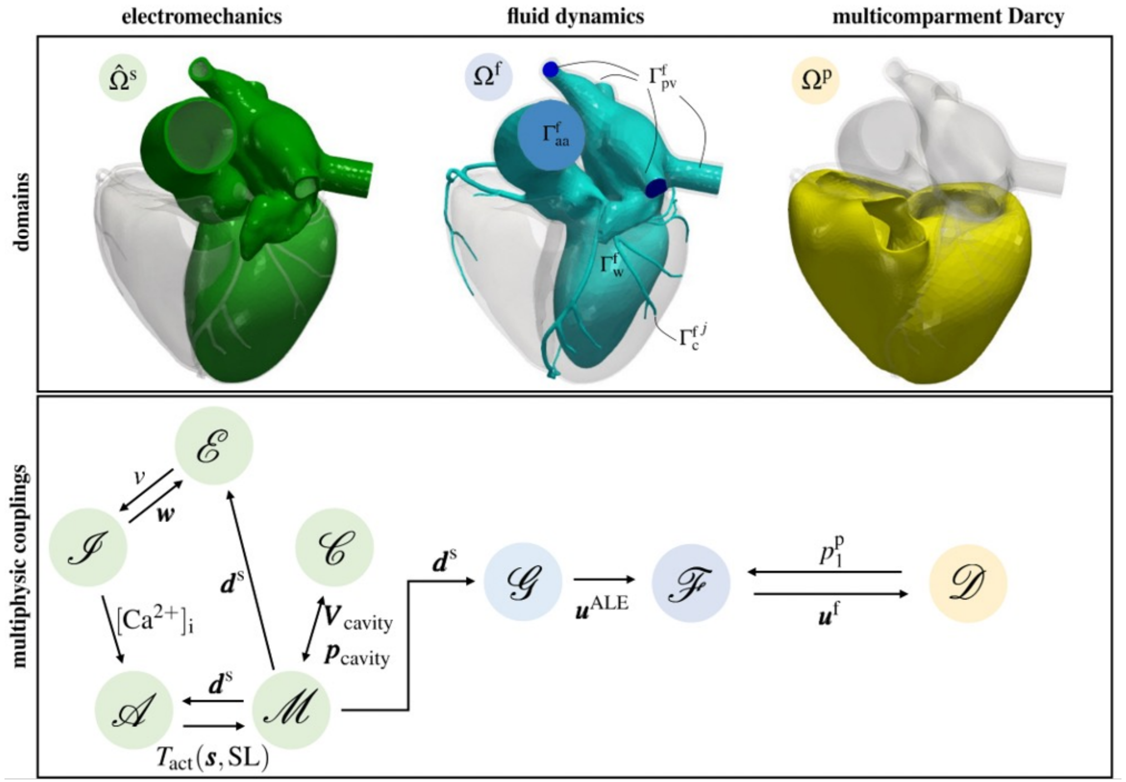

- **Electromechanics** of the left heart
- Blood **fluid dynamics** in left heart and large epicardial coronaries
- **Valves** modeled with RIIS method
- **Multicompartment Darcy model** for myocardial perfusion

- One-way EM-CFD
- Fully coupled CFD-Multicompartment Darcy

A. Zingaro, C. Vergara, L. Dede', F. Regazzoni, A. Quarteroni, arXiV (2023)

Electromechanics driven CFD-Darcy model for perfusion

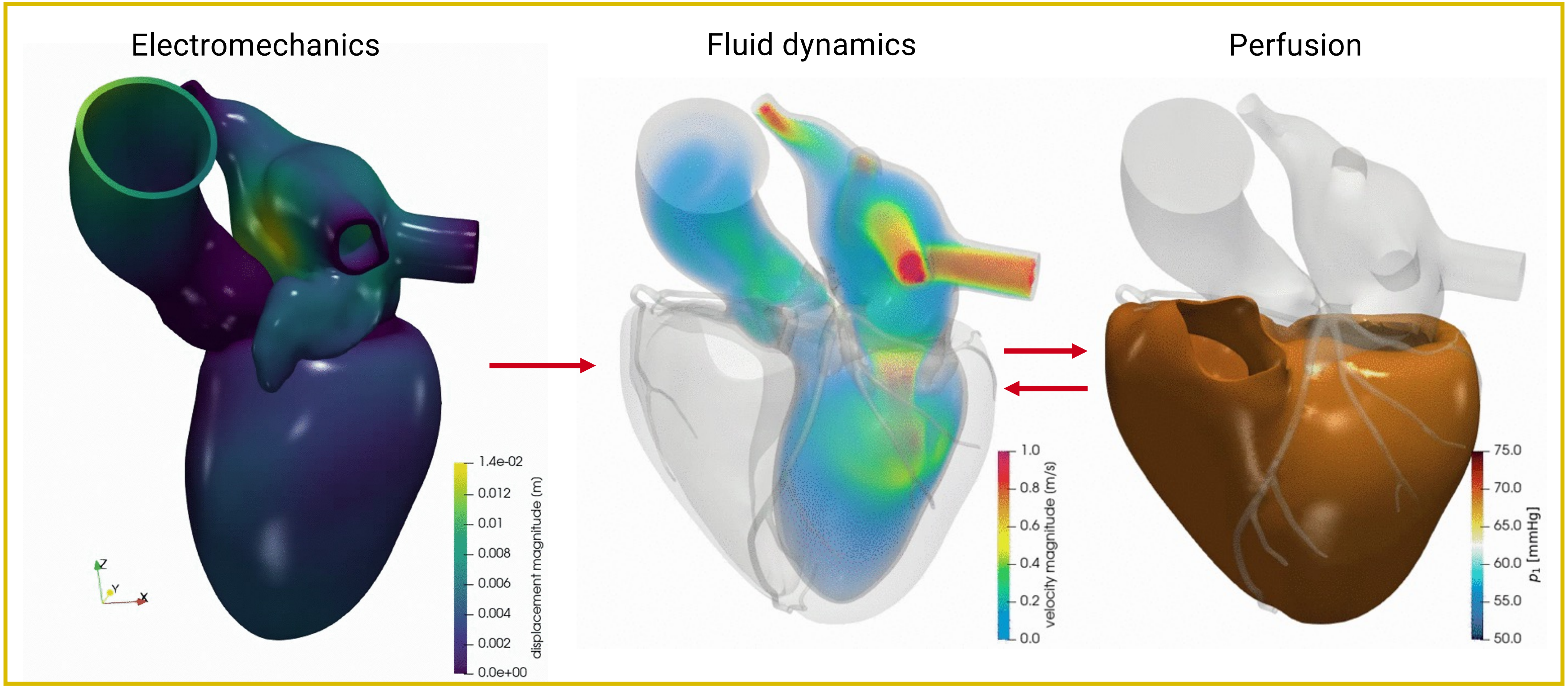

A. Zingaro, C. Vergara, L. Dede', F. Regazzoni, A. Quarteroni, arXiV (2023)

A lumped model for the circulatory system

$$\mathbf{F}_{\text{circ}}\left(\mathbf{c}, \frac{\mathrm{d}\mathbf{c}}{\mathrm{d}t}, t\right) = \mathbf{0}$$

Unknowns

$\mathbf{c}$: Circulation state (pressure, flowrate, chamber volume)

- **ordinary differential-algebraic** system
- **electric circuit analogy**
- **modular coupling** with 3D models (either mechanics or fluid dynamics)

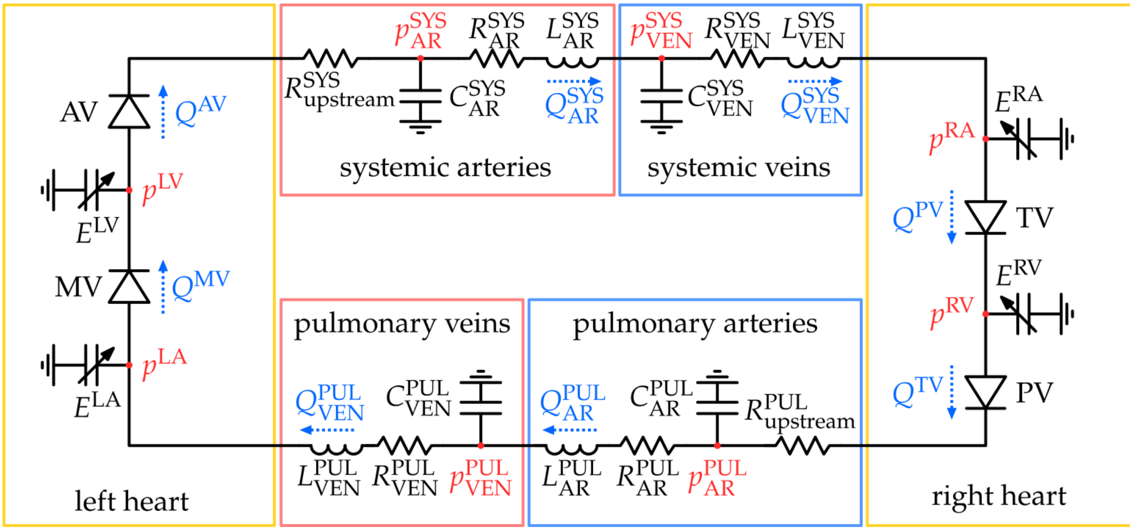

F. Regazzoni, M. Salvador, P. C. Africa, et al., *Journal of Computational Physics*, 2022
M. Hirschvogel, M. Bassilious, M. Jagschies, et al., *Inernational Journal for Numerical Methods in Biomedical Engineering*, 2017

Numerical generation of 12-lead ECG system

$$
\begin{cases}
\mathrm{EP}(v, v_e) = 0 & \text{in } \Omega_H \\
-\nabla \cdot (D_T \nabla v_T) = 0 & \text{in } \Omega_{\text{torso}} \\
v_T = v_e & \text{on } \Sigma \\
D_T \nabla v_T \cdot \mathbf{n}_H = D_e \nabla v_e \cdot \mathbf{n}_H & \text{on } \Sigma
\end{cases}
$$

Unknowns

v_T : extra-cellular potential in torso

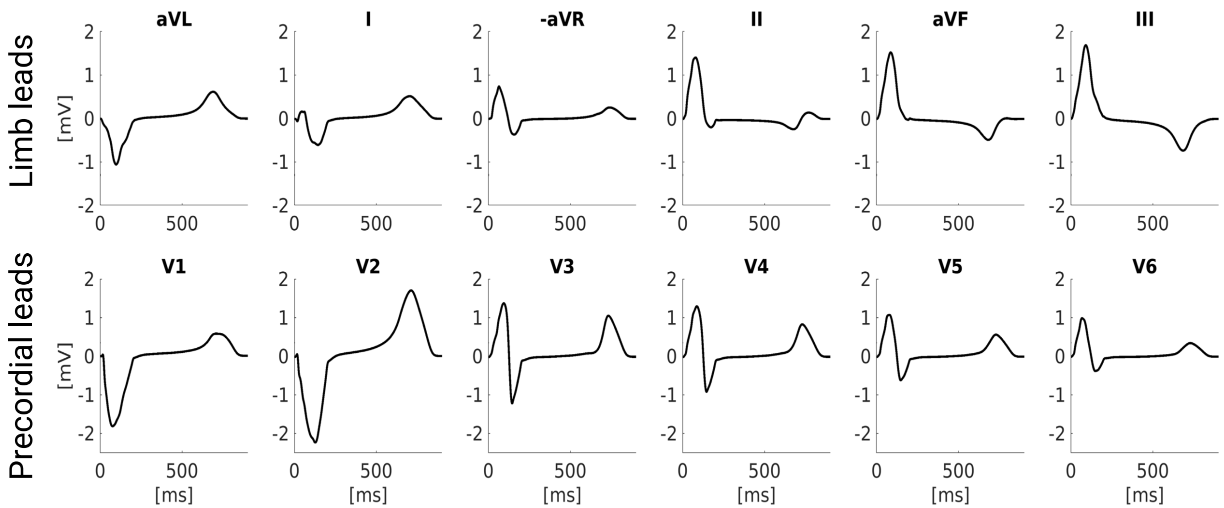

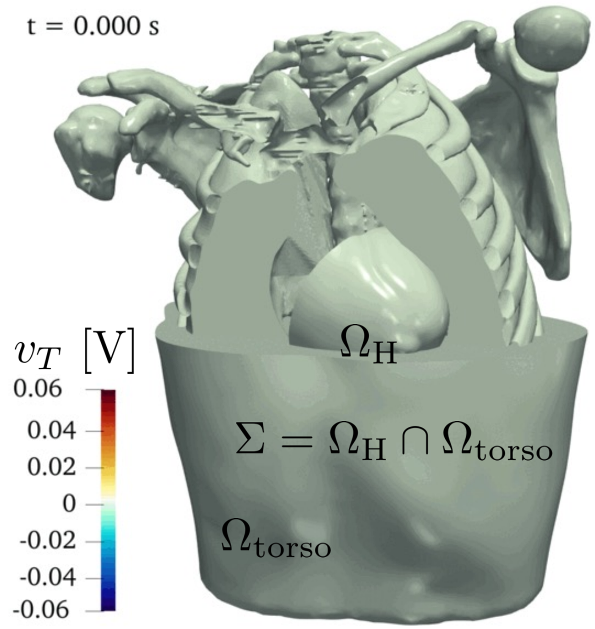

Minor inconsistencies in T-wave due to lack of ionic heterogeneity

M. Boulakia, S. Cazeau, M.A. Fernández, et al., *Annals of Biomedical Engineering*, 2010
E. Zappon, et al., *MOX Report*, Politecnico di Milano, 2022

The Integrated Mathematical Heart (the Core Equations)

$$\begin{cases} \dfrac{\partial \mathbf{w}}{\partial t} = \mathbf{F}^{\mathbf{w}}_{\mathrm{ion}}(v, \mathbf{w}) & \text{in } \Omega \\ \dfrac{\partial \mathbf{z}}{\partial t} = \mathbf{F}^{\mathbf{z}}_{\mathrm{ion}}(v, \mathbf{w}, \mathbf{z}) & \text{in } \Omega \end{cases}$$

Cellular Ions' dynamics

$$\begin{cases} J\chi C_{\mathrm{m}} \dfrac{\partial v}{\partial t} - \nabla \cdot (J F^{-1} D_{\mathrm{i}} F^{-T} \nabla (v + v_{\mathrm{e}})) + J\chi I_{\mathrm{ion}}(v, \mathbf{w}, \mathbf{z}) = J\chi I_{\mathrm{app}}(\mathbf{x}, t) & \text{in } \Omega \\ -\nabla \cdot (J F^{-1} D_{\mathrm{i}} F^{-T} \nabla v) - \nabla \cdot (J F^{-1} (D_{\mathrm{i}} + D_{\mathrm{e}}) \nabla v_{\mathrm{e}}) = 0 & \text{in } \Omega \end{cases}$$

Electrophysiology

$$\mathbf{F}_{\mathrm{circ}}\left(\mathbf{c}, \frac{\mathrm{d}\mathbf{c}}{\mathrm{d}t}, t\right) = \mathbf{0}$$

External Circulation

$$\begin{cases} \dfrac{\partial \mathbf{s}}{\partial t} = \mathbf{F}_{\mathrm{act}}\left(\mathbf{s}, [\mathrm{Ca}^{2+}]_{\mathrm{i}}, \mathrm{SL}, \dfrac{\partial \mathrm{SL}}{\partial t}\right) & \text{in } \Omega \\ \mathrm{SL} = \mathrm{SL}_0 \sqrt{I_{4\mathrm{f}}} & \text{in } \Omega \end{cases}$$

$$P_{\mathrm{act}}(\mathbf{d}, \mathbf{s}) = T_{\mathrm{act}} \left(n_{\mathrm{f}} \frac{F\mathbf{f}_0 \cdot \mathbf{f}_0}{\sqrt{I_{4\mathrm{f}}}} + n_{\mathrm{s}} \frac{F\mathbf{s}_0 \cdot \mathbf{s}_0}{\sqrt{I_{4\mathrm{s}}}} + n_{\mathrm{n}} \frac{F\mathbf{n}_0 \cdot \mathbf{n}_0}{\sqrt{I_{4\mathrm{n}}}} \right)$$

$$T_{\mathrm{act}} = T_{\mathrm{act}}(\mathbf{s}, \mathrm{SL}), \qquad I_{4\mathrm{i}} = F\mathbf{i}_0 \cdot F\mathbf{i}_0 \quad \mathrm{i} \in \{\mathbf{f}, \mathbf{s}, \mathbf{n}\}$$

Cardiomyocites Contraction

$$\begin{cases} \mathrm{NS}(\mathbf{u}, p) = \mathbf{0} & \text{in } \Omega_{\mathrm{cor}} \\ \mathbf{K}_i^{-1} \mathbf{u}_{\mathrm{myo},i} + \nabla p_{\mathrm{myo},i} = \mathbf{0}, \quad i = 1, 2, 3 & \text{in } \Omega_{\mathrm{myo}} \\ \nabla \cdot \mathbf{u}_{\mathrm{myo},1} = \displaystyle\sum_{j=1}^{J} \frac{\chi_{\Omega^j_{\mathrm{myo}}}}{|\Omega^j_{\mathrm{myo}}|} \int_{\Gamma^{\mathrm{coro}}_j} \mathbf{u} \cdot \mathbf{n} - \beta_{1,2}(p_{\mathrm{myo},1} - p_{\mathrm{myo},2}) & \text{in } \Omega_{\mathrm{myo}} \\ \nabla \cdot \mathbf{u}_{\mathrm{myo},2} = -\beta_{2,1}(p_{\mathrm{myo},2} - p_{\mathrm{myo},1}) - \beta_{2,3}(p_{\mathrm{myo},2} - p_{\mathrm{myo},3}) & \text{in } \Omega_{\mathrm{myo}} \\ \nabla \cdot \mathbf{u}_{\mathrm{myo},3} = -\gamma(p_{\mathrm{myo},3} - p_{\mathrm{veins}}) - \beta_{3,2}(p_{\mathrm{myo},3} - p_{\mathrm{myo},2}) & \text{in } \Omega_{\mathrm{myo}} \end{cases}$$

Myocardial Perfusion

$$\rho_{\mathrm{f}} \left[\frac{\partial \mathbf{u}}{\partial t} + ((\mathbf{u} - \mathbf{u}_{\mathrm{ALE}}) \cdot \nabla)\, \mathbf{u} \right] - \nabla \cdot \sigma_{\mathrm{f}}(\mathbf{u}, p) + \boldsymbol{\mathcal{R}}(\mathbf{u}, \mathbf{u}_{\mathrm{ALE}}) = \mathbf{0}$$

$$\boldsymbol{\mathcal{R}}(\mathbf{u}, \mathbf{u}_{\mathrm{ALE}}) = \sum_{\mathrm{k} \in \mathcal{V}} \frac{R_{\mathrm{k}}}{\varepsilon_{\mathrm{k}}} \delta_{\varepsilon_{\mathrm{k}}} \left(\varphi^t_{\mathrm{k}}(\mathbf{x}) \right) (\mathbf{u} - \mathbf{u}_{\mathrm{ALE}} - \mathbf{u}_{\Gamma_{\mathrm{k}}})$$

Valves Dynamics

$$\begin{cases} -\nabla \cdot P_{\mathrm{ALE}}(\mathbf{d}_{\mathrm{ALE}}) = \mathbf{0} & \text{in } \widehat{\Omega} \\ \mathbf{d}_{\mathrm{ALE}} = \mathbf{d} & \text{on } \hat{\Sigma} \end{cases} \qquad \mathbf{u}_{\mathrm{ALE}} = \frac{\partial \mathbf{d}_{\mathrm{ALE}}}{\partial t}$$

$$\begin{cases} \rho_{\mathrm{f}} \left[\dfrac{\partial \mathbf{u}}{\partial t} + ((\mathbf{u} - \mathbf{u}_{\mathrm{ALE}}) \cdot \nabla)\, \mathbf{u} \right] - \nabla \cdot \sigma_{\mathrm{f}}(\mathbf{u}, p) = \mathbf{0} & \text{in } \Omega \\ \nabla \cdot \mathbf{u} = 0 & \text{in } \Omega \end{cases}$$

$$\sigma_{\mathrm{f}}(\mathbf{u}, p) = \mu \left(\nabla \mathbf{u} + \nabla \mathbf{u}^T \right) - pI$$

Blood Dynamics, Contraction & Relaxation

$$\rho_{\mathrm{s}} \frac{\partial^2 \mathbf{d}}{\partial t^2} - \nabla \cdot P_{\mathrm{s}}(\mathbf{d}, \mathbf{s}) = \mathbf{0} \qquad \text{in } \Omega$$

$$P_{\mathrm{s}}(\mathbf{d}, \mathbf{s}) = P_{\mathrm{pas}}(\mathbf{d}) + P_{\mathrm{act}}(\mathbf{d}, \mathbf{s})$$

$$P_{\mathrm{pas}}(\mathbf{d}) = \frac{\partial \mathcal{W}}{\partial F} \qquad F = I + \nabla \mathbf{d}$$

ECG Reconstruction

$$\begin{cases} \mathrm{EP}(v, v_e) = 0 & \text{in } \Omega_H \\ -\nabla \cdot (D_T \nabla v_T) = 0 & \text{in } \Omega_{\mathrm{torso}} \\ v_T = v_e & \text{on } \Sigma \\ D_T \nabla v_T \cdot \mathbf{n}_H = D_e \nabla v_e \cdot \mathbf{n}_H & \text{on } \Sigma \end{cases}$$

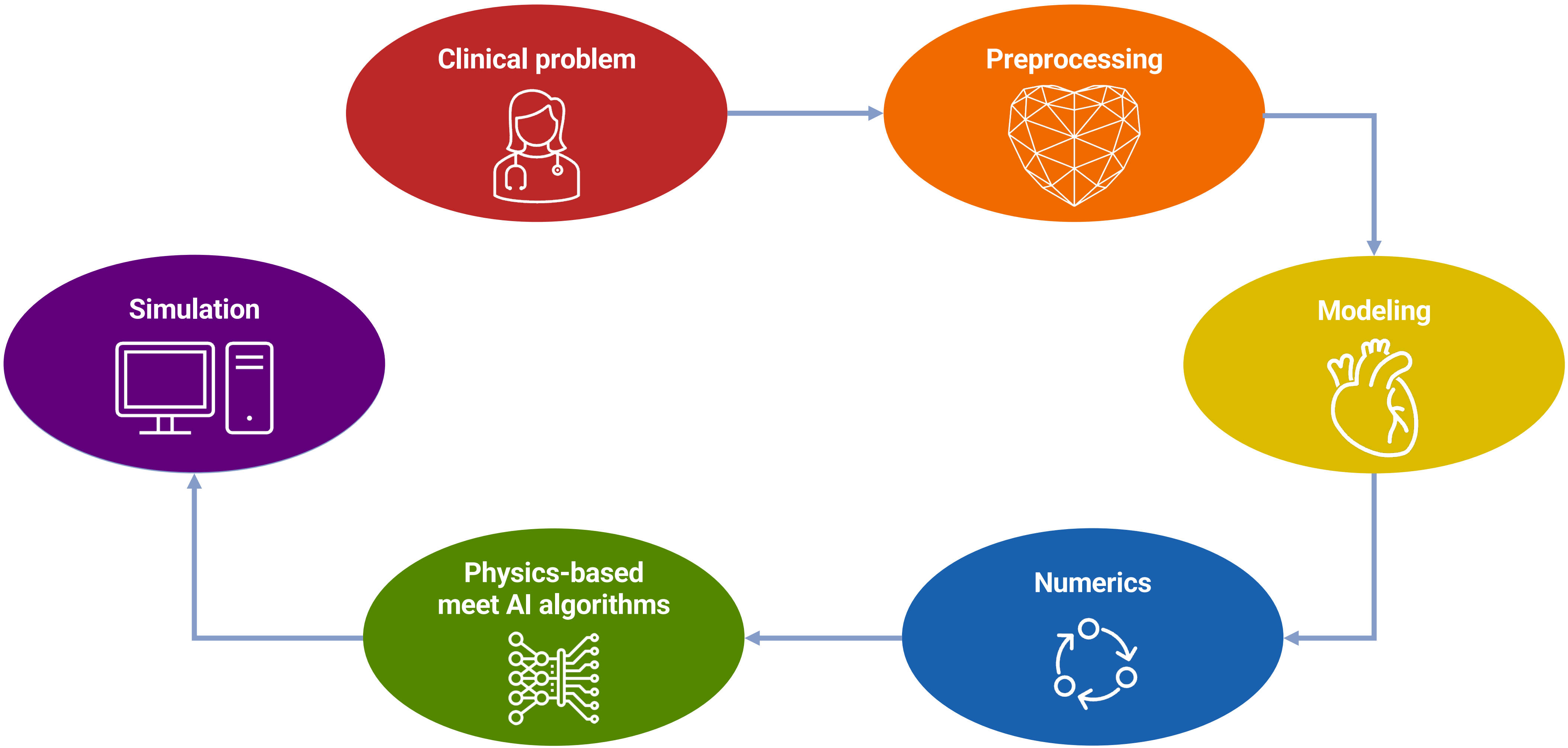
Clinical problem
Preprocessing
Modeling
Numerics
Physics-based
meet AI algorithms
Simulation

Whole heart electrophysiology

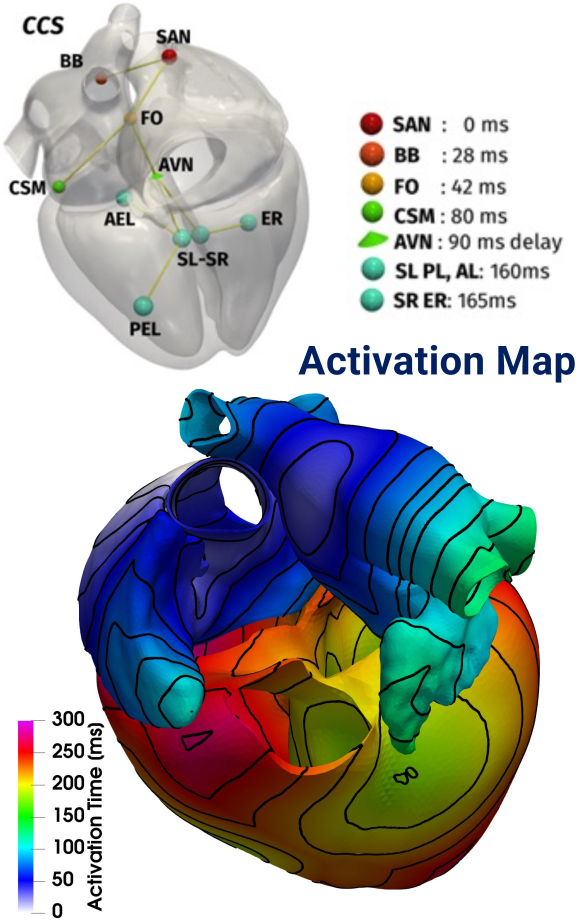

- Cardiac Conduction System (CCS) as a series of delayed stimuli
- Monodomain + TTP06 (ventricles) and CRN98 (atria)
- Whole heart fibers using LDRBM

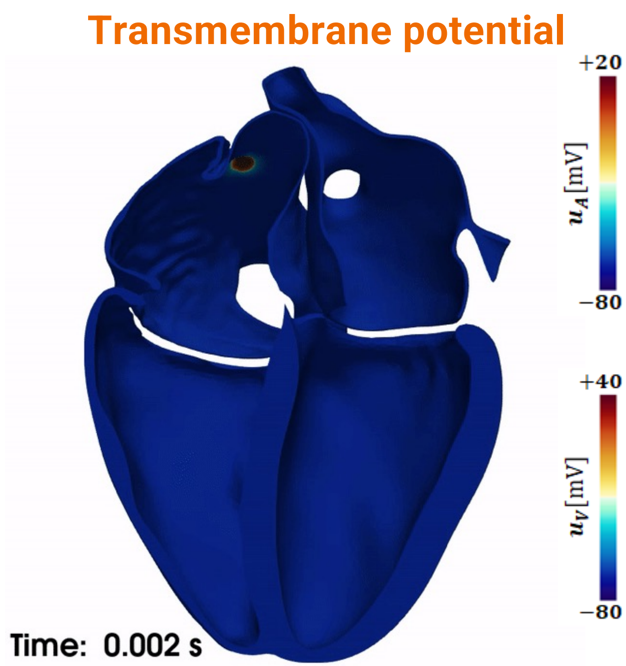

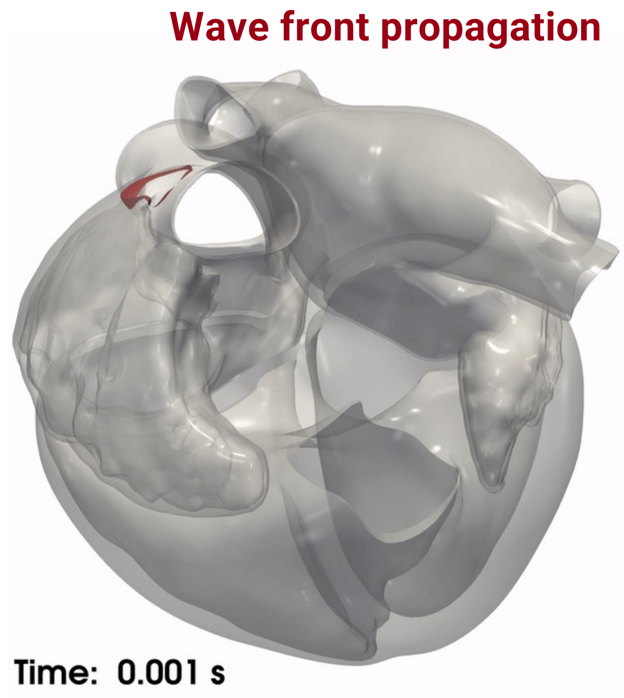

R. Piersanti, P. Africa, M. Fedele et al., *Computer Methods in Applied Mechanics and Engineering*, 2021

Results: 4CH with tuned RQD20MF + improvements

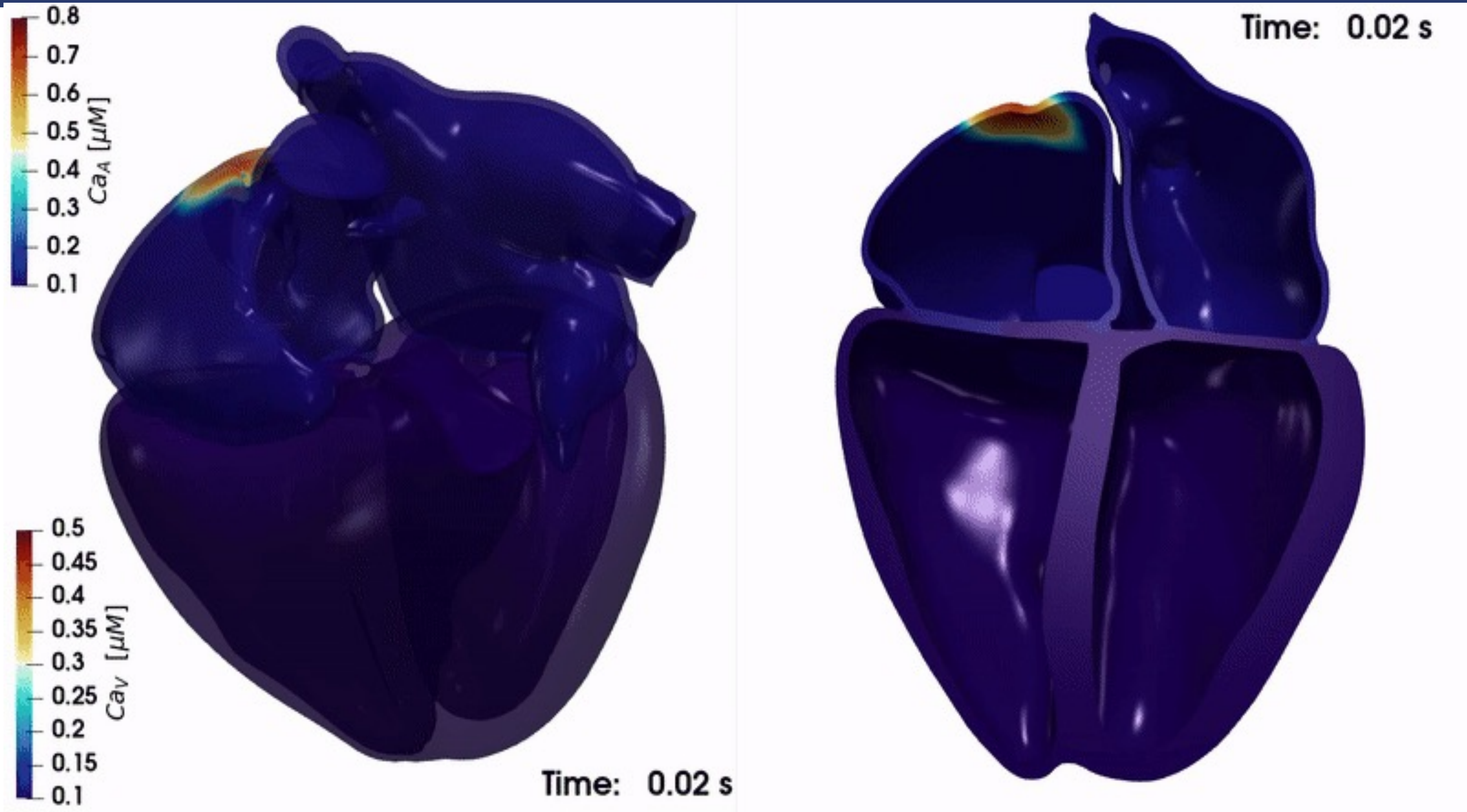

The Active Tension

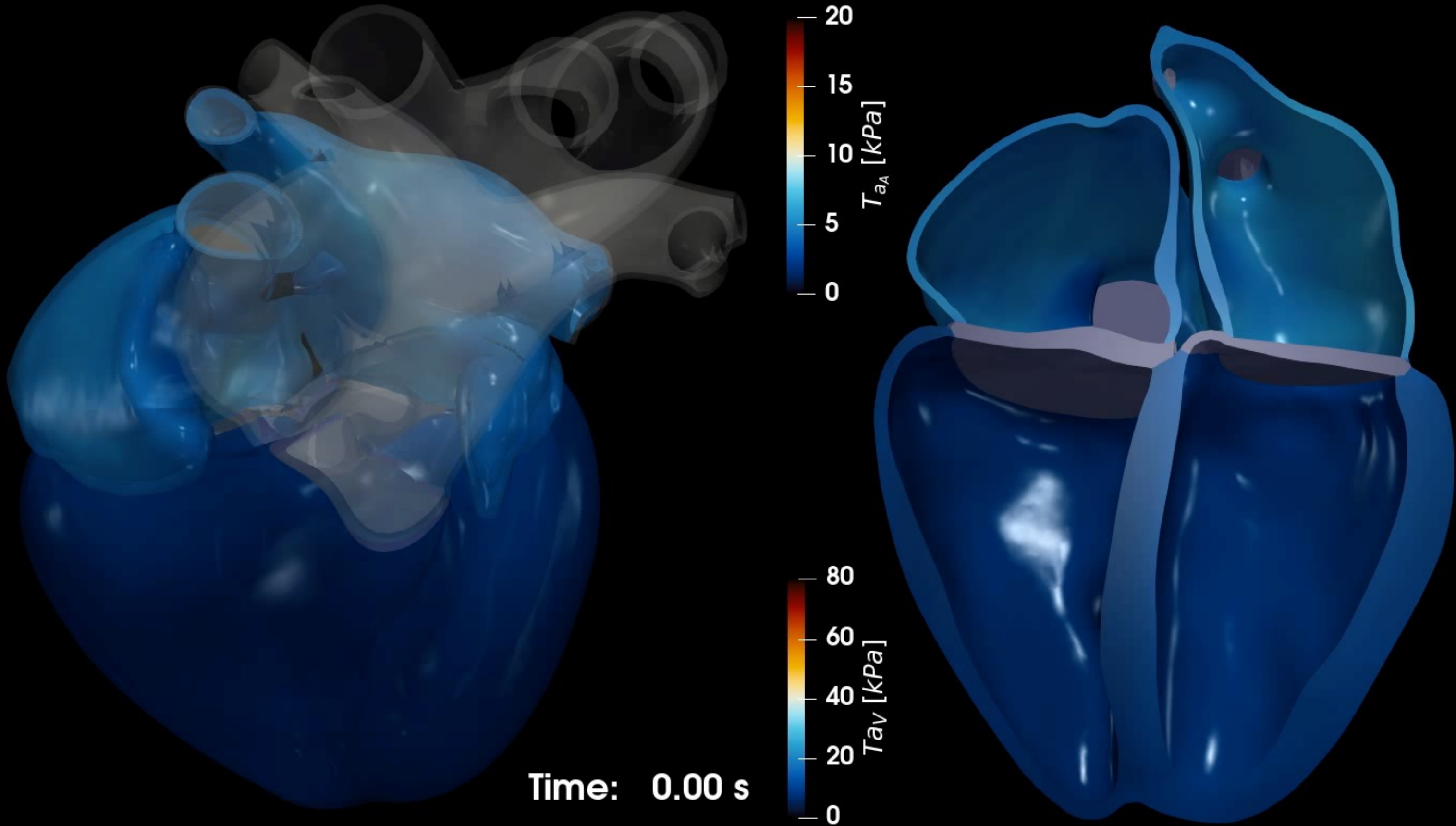

The Displacement

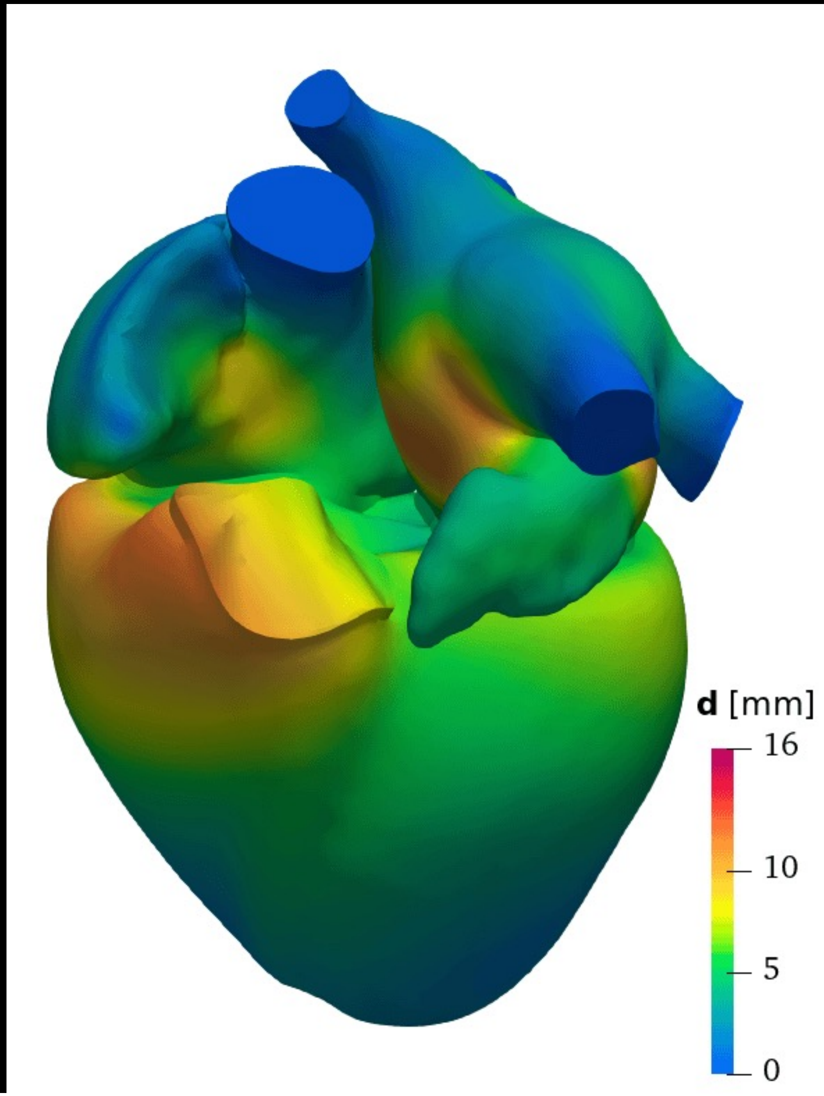

Fluid dynamics of the left heart (A.Zingaro)

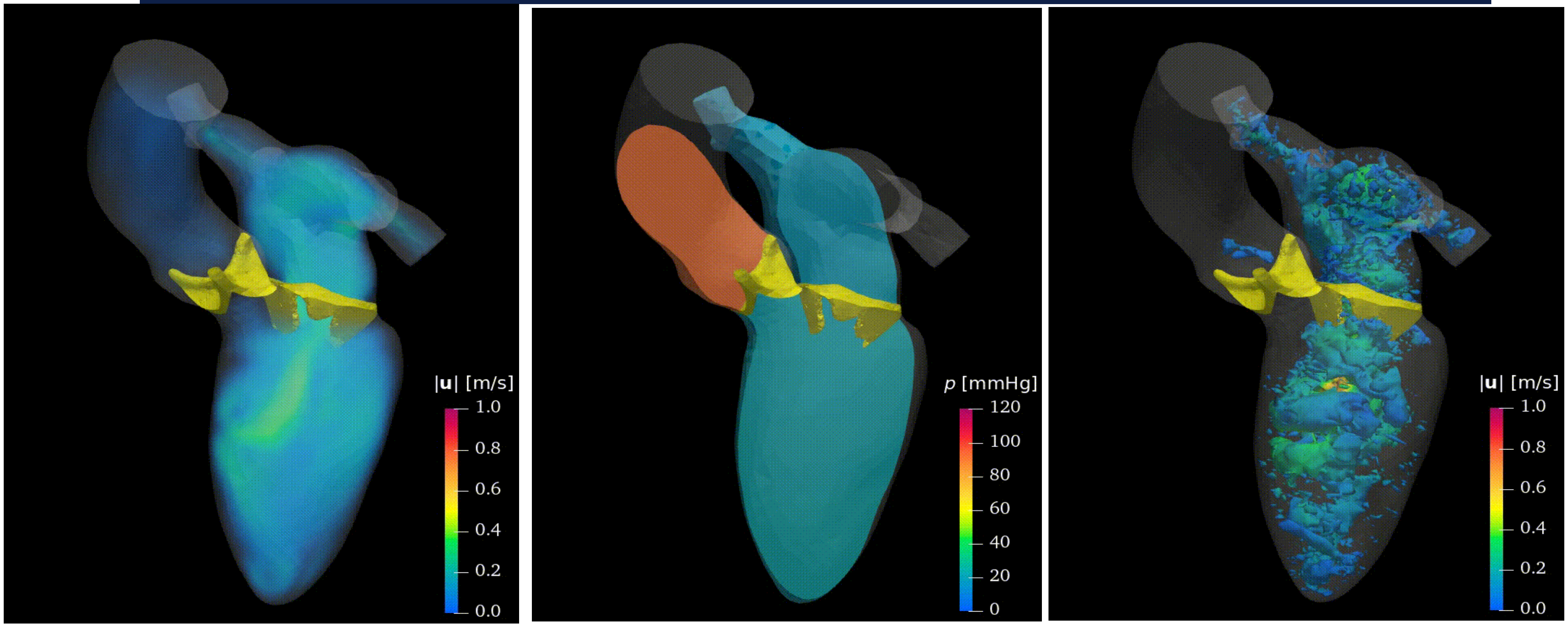

Q-criterion and velocity magnitude:

- when the mitral valve opens, high speed jets coming from the LA fill the LV.
- This produces the formation of a O-ring shaped vortex, a coherent structure rolling through the leaflets of the mitral valve.
- This big vortex breaks into smaller coherent structures filling the LV and moving towards the apex.
- As the systole begins, marked by the opening of the aortic valve, the structures are flushed out in the aorta.
- At the same time, new jets are entering in the LA, but weaker with respect to the ones observed in diastole.

Electromechanics driven CFD-Darcy model for perfusion

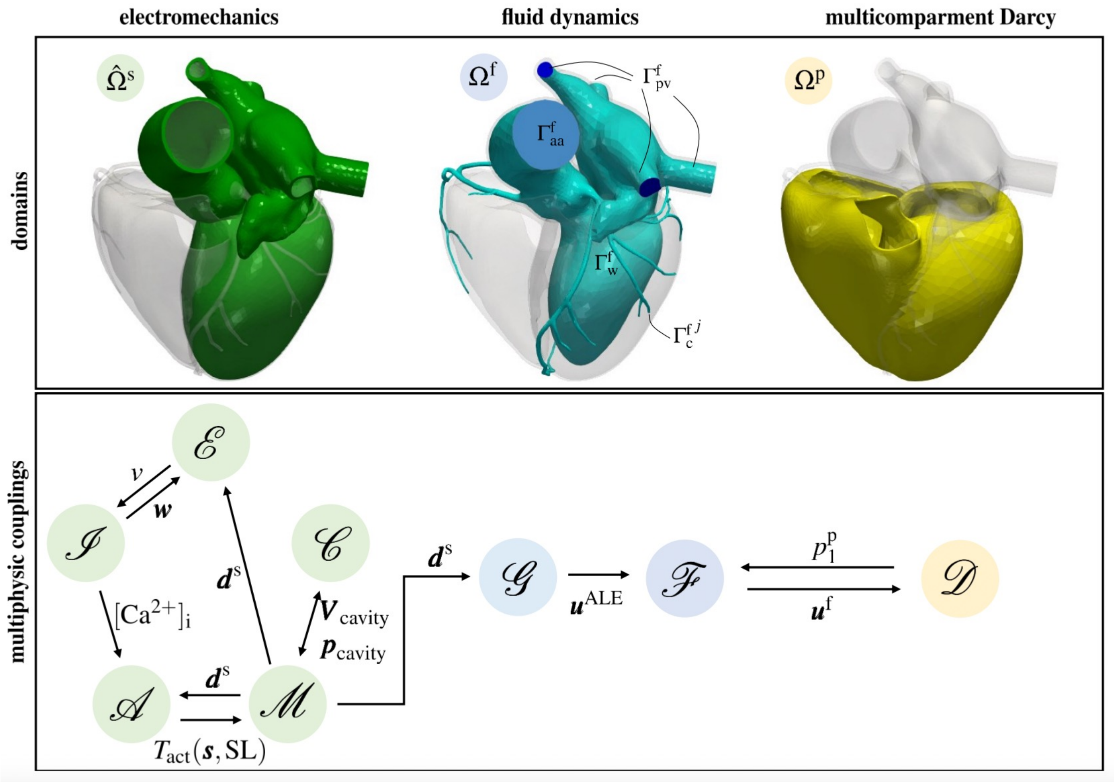

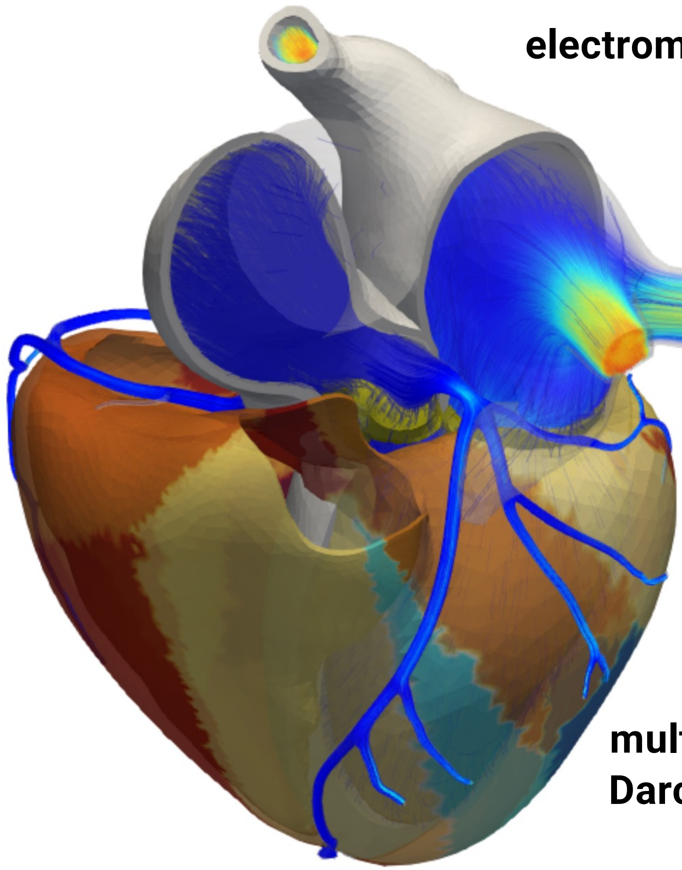

A. Zingaro, C. Vergara, L. Dede', F. Regazzoni, A. Quarteroni, arXiV (2023)

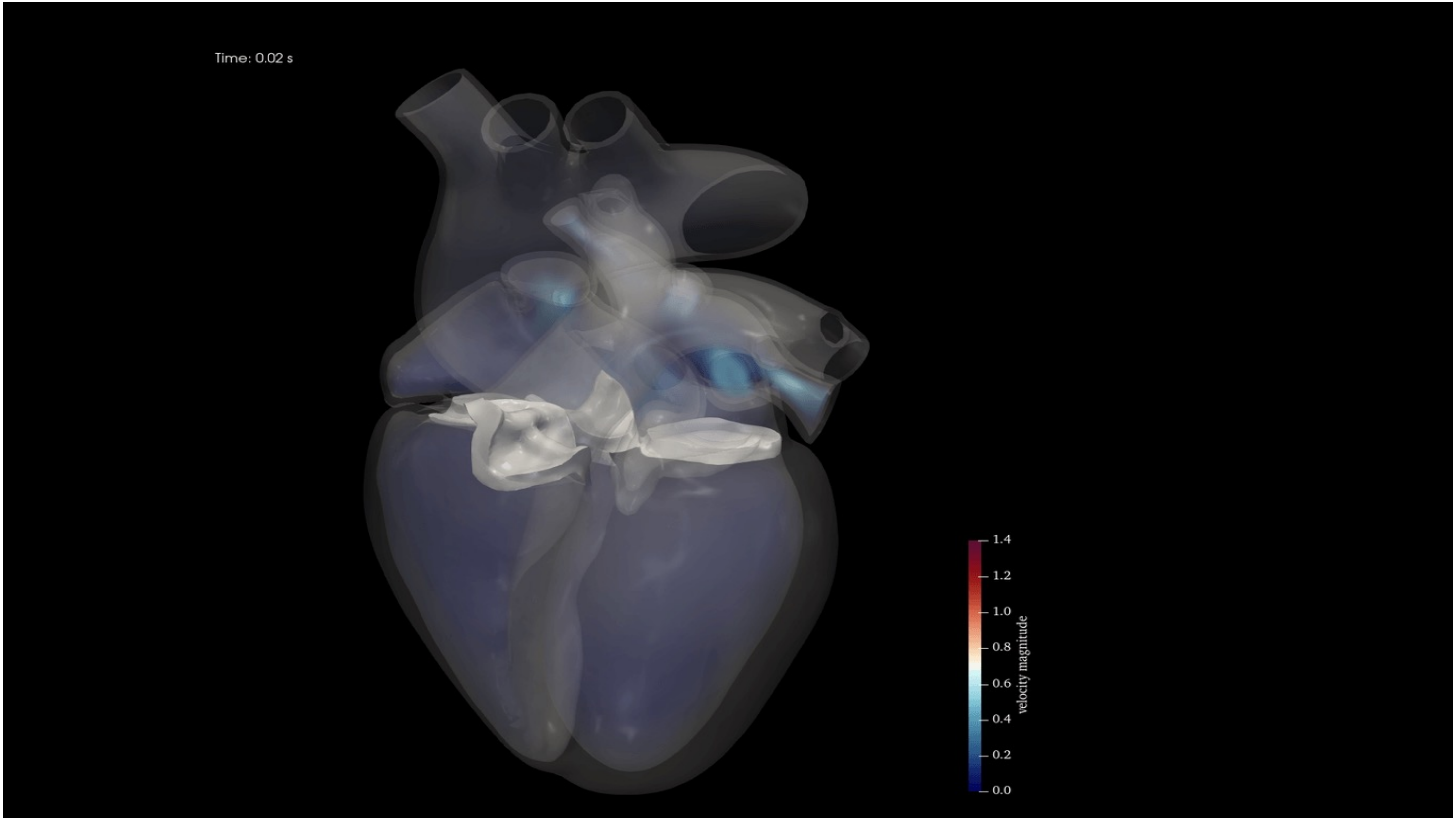
Time: 0.02 s
1.4
1.2
1.0
0.8
0.6
0.4
0.2
0.0
velocity magnitude

Electromechanics driven CFD-Darcy model for perfusion

Modeling

A physiological simulation

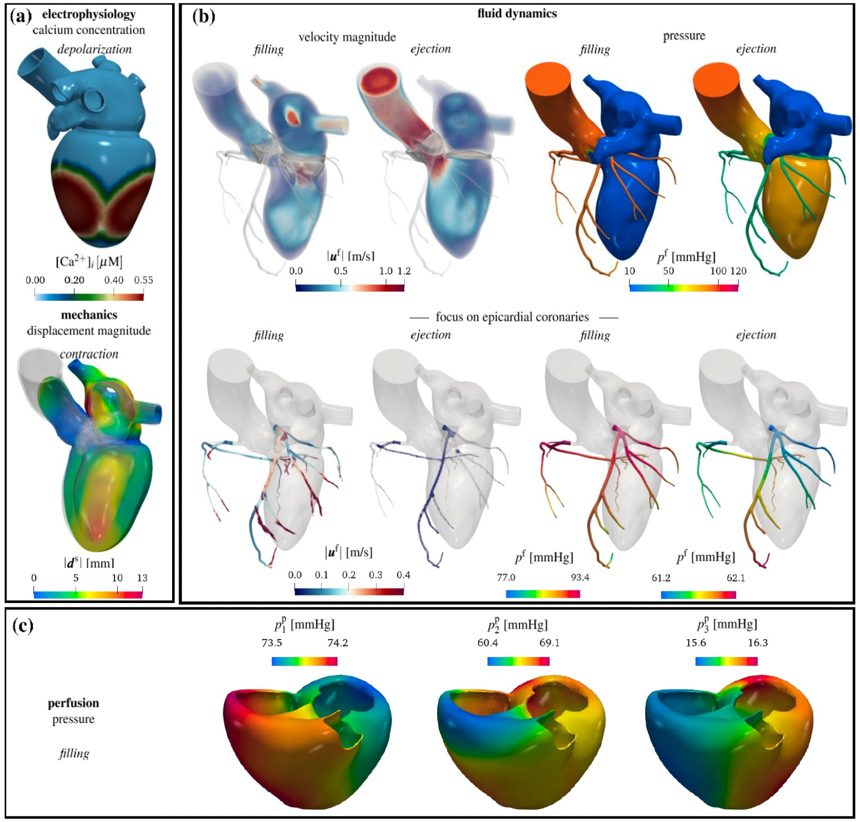

Consequences of aortic regurgitation (AR) on myocardial perfusion

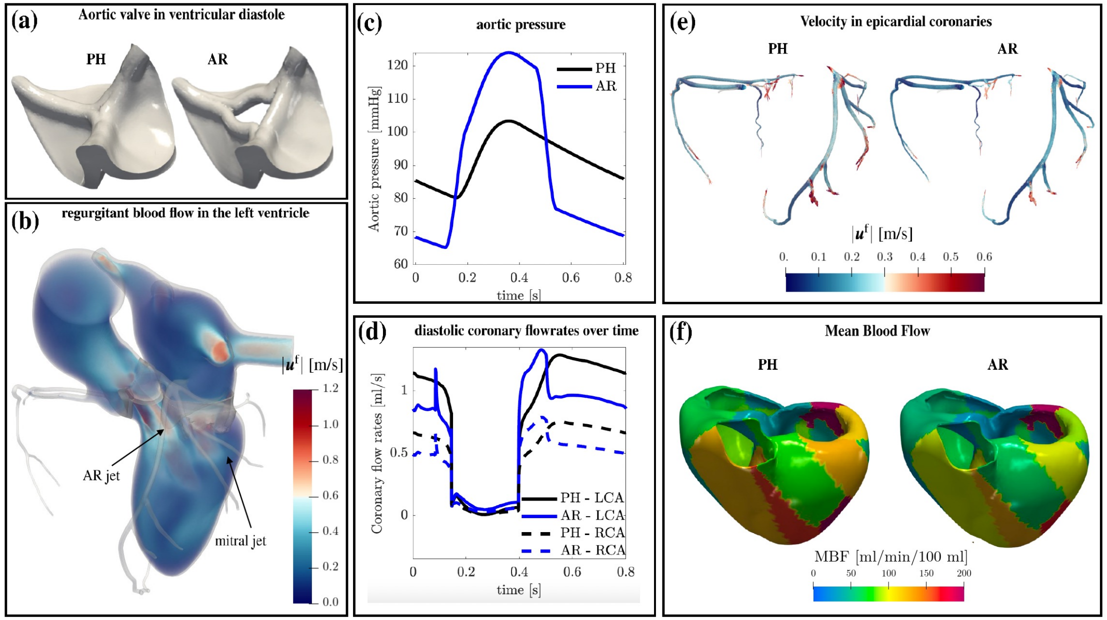

Diastolic coronary blood flow stolen by the LV (due to AR)

Reduced MBF in AR case!

A. Zingaro, C. Vergara, L. Dede', F. Regazzoni, A. Quarteroni, arXiV (2023)

A complete simulation of a single heartbeat

Requires at least 1.7M nodes, 20M degrees of freedom for PDEs, around 31M for ODEs, 16K timesteps: in total, 700B variables for the space-time solver on 1152 cores on the supercomputer GALILEO @ CINECA

Takes 4 hours

Costs about 2000 euros

Consumes 100kWh of energy

Produces 35kg of CO_2 (without accounting for the additional CO_2 produced for the cooling of the cluster)

Developing better models and more efficient and accurate numerical methods is of paramount importance

we need

a **BETTER MATH**

For a **SUSTAINABLE WORLD**

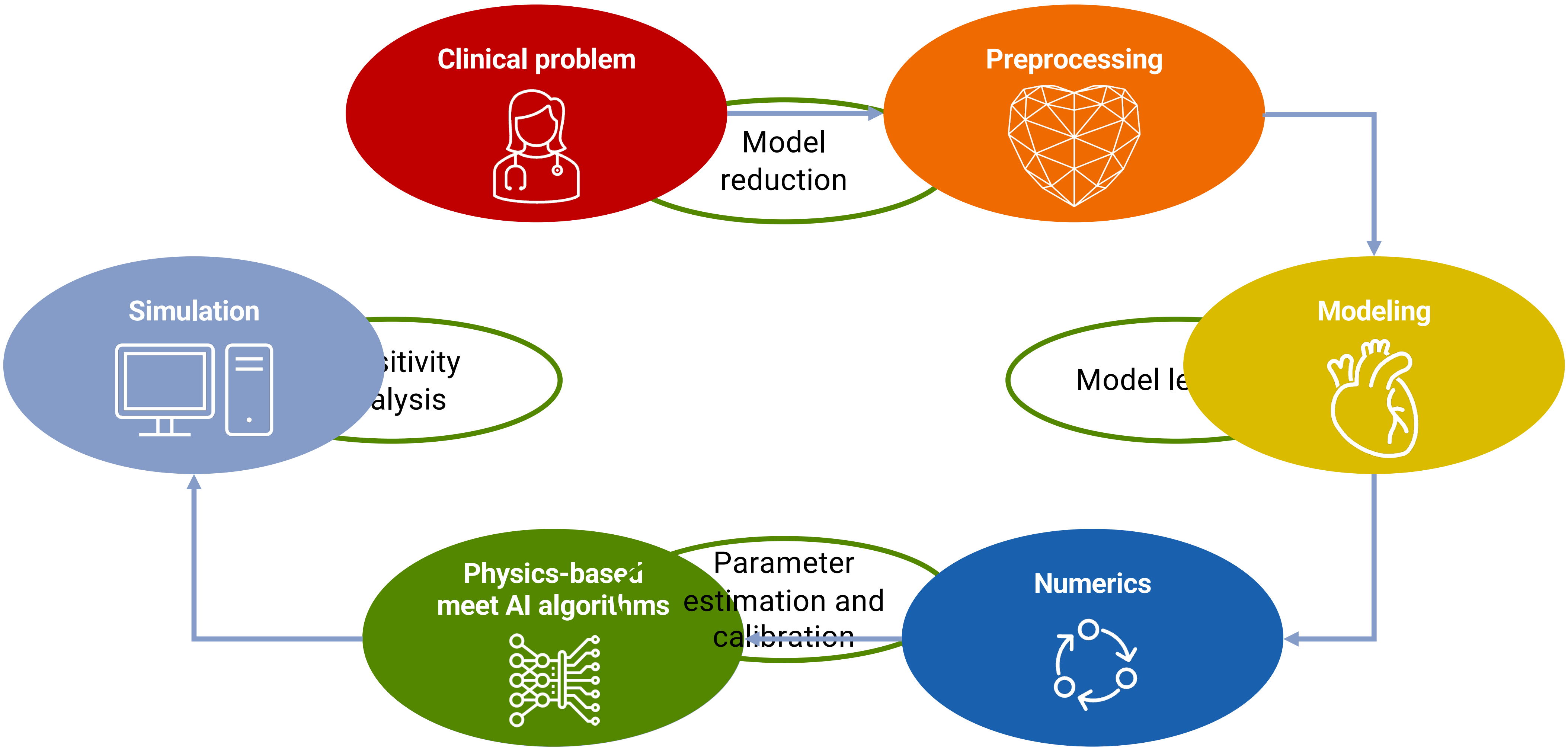
Clinical problem
Preprocessing
Model
reduction
Simulation
itivity
alysis
Model le
Modeling
Physics-based
meet AI algorithms
Parameter
estimation and
calibration
Numerics

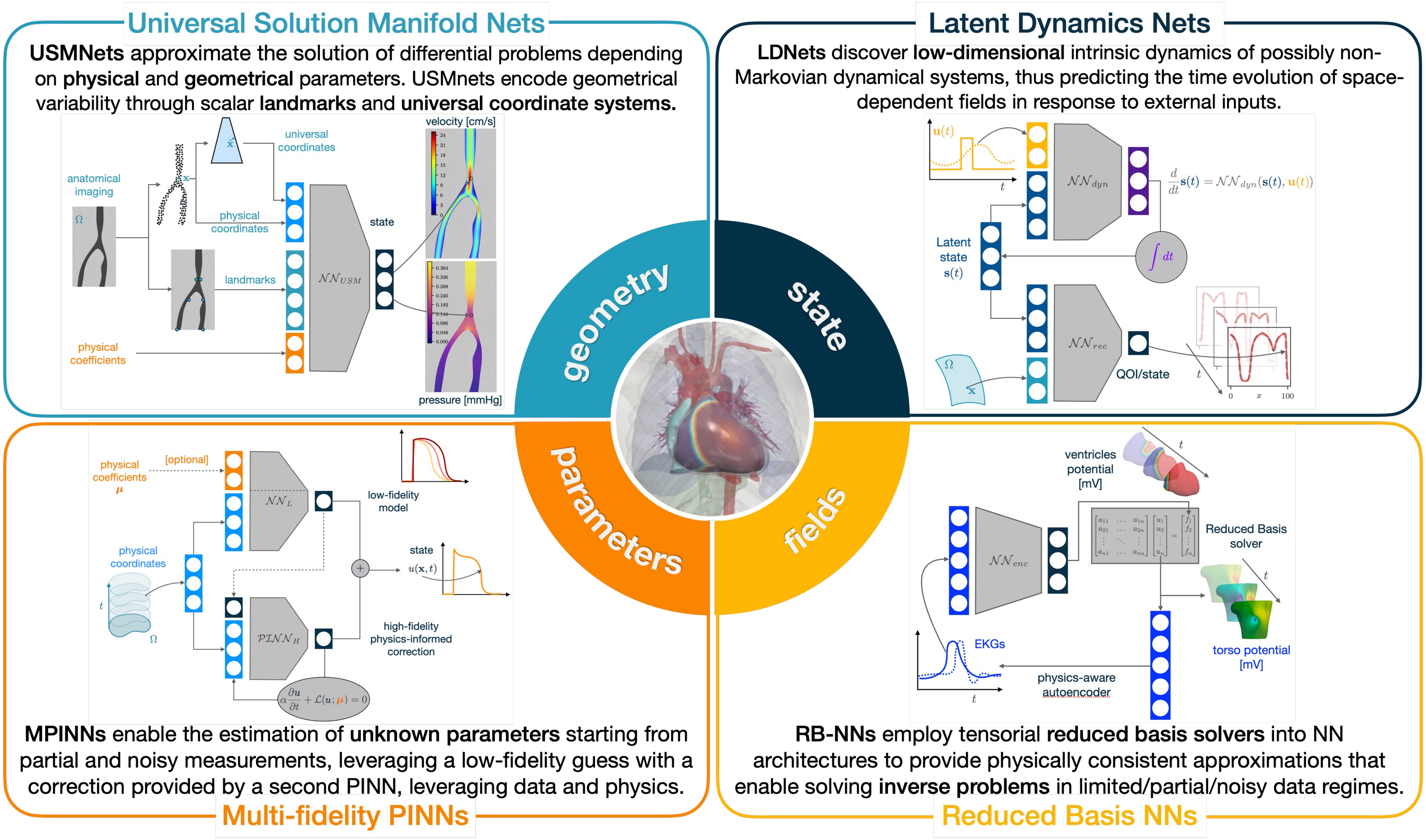

Universal Solution Manifold Nets
USMNets approximate the solution of differential problems depending on physical and geometrical parameters. USMnets encode geometrical variability through scalar landmarks and universal coordinate systems.
anatomical imaging
universal coordinates
physical coordinates
landmarks
physical coefficients
state
velocity [cm/s]
pressure [mmHg]
Latent Dynamics Nets
LDNets discover low-dimensional intrinsic dynamics of possibly non-Markovian dynamical systems, thus predicting the time evolution of space-dependent fields in response to external inputs.
Latent state
QOI/state
geometry
state
parameters
fields
physical coefficients
[optional]
low-fidelity model
physical coordinates
state
high-fidelity physics-informed correction
MPINNs enable the estimation of unknown parameters starting from partial and noisy measurements, leveraging a low-fidelity guess with a correction provided by a second PINN, leveraging data and physics.
Multi-fidelity PINNs
ventricles potential [mV]
Reduced Basis solver
EKGs
physics-aware autoencoder
torso potential [mV]
RB-NNs employ tensorial reduced basis solvers into NN architectures to provide physically consistent approximations that enable solving inverse problems in limited/partial/noisy data regimes.
Reduced Basis NNs

Learning the dynamics of active force generation

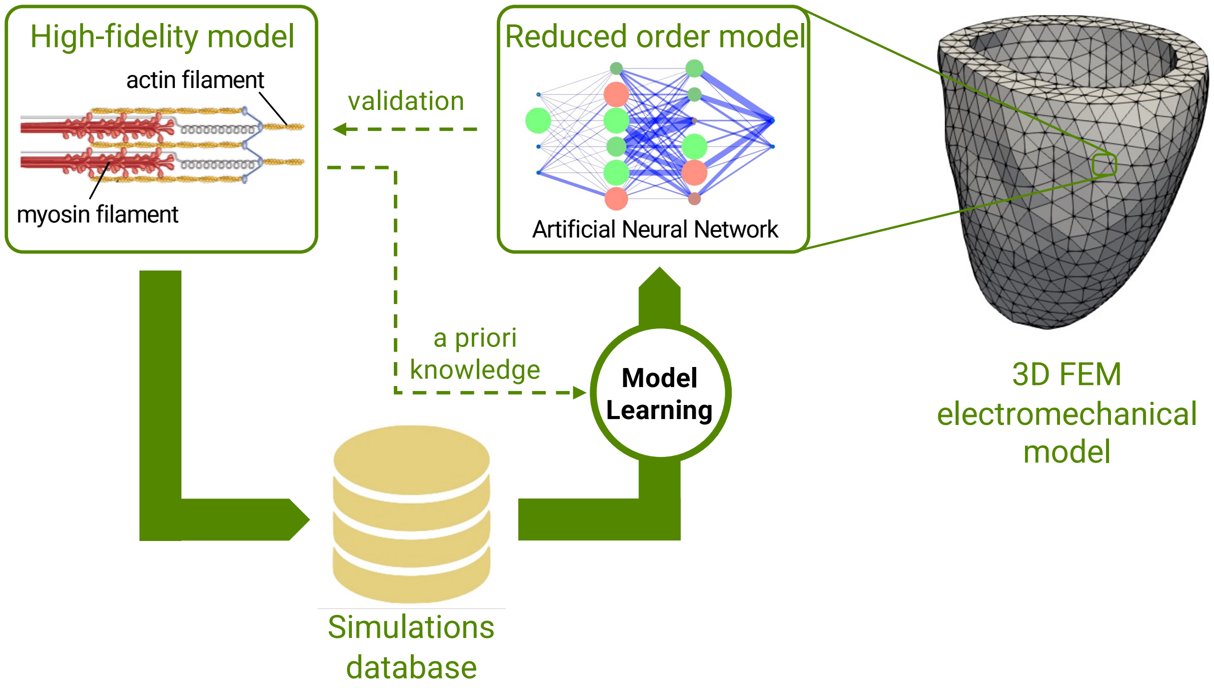

- ✓ 400x speedup (force generation model)
- ✓ 10x speedup (overall)
- ✓ 100x memory saving

Accuracy

Indicator	HF-EM	ANN-EM	Relative error
Stroke volume (mL)	58.45	58.42	$5.64 \cdot 10^{-4}$
Ejection fraction (%)	43.03	43.01	$5.65 \cdot 10^{-4}$
Max pressure (mmHg)	112.5	112.3	$2.18 \cdot 10^{-3}$
Work (mJ)	739.2	737.2	$1.71 \cdot 10^{-3}$

Computational time (20 cores)

	Ionic	Potential	Force gen.	Mechanics	Total
HF-EM	3.13 %	0.47 %	83.07 %	13.33 %	20h 18’
ANN-EM	41.21 %	4.80 %	2.54 %	51.45 %	2h’ 03’

Memory usage

from 2198 (HF-EM) to 24 (ANN-EM) variables per nodal point

F. Regazzoni, L. Dede’, A. Q., *Journal of Computational Physics*, 2019
F. Regazzoni, L. Dede’, A. Q., *Computer Methods in Applied Mechanics and Engineering*, 2020

Multi-fidelity PINNs for the estimation of ionic parameters

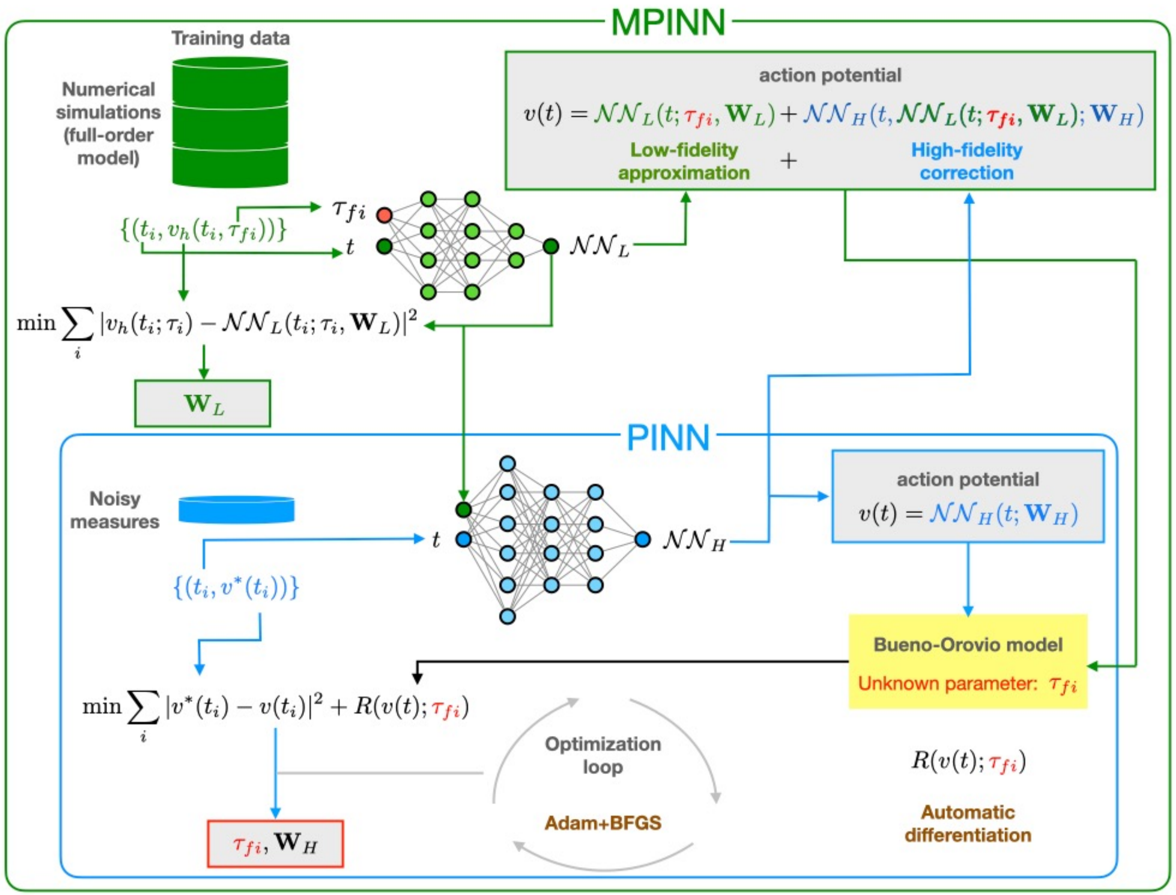

Goal: estimate the parameter τ_{fi} of the Bueno-Orovio model (time constant of fast inward current) from transmembrane potential noisy measurements

Method: train a **multi-fidelity PINN** minimizing a loss function weighing:

- discrepancy from a low-fidelity model (e.g. a second ANN, trained on precomputed **numerical data**)
- discrepancy from **noisy observations**
- residual of the differential equations (**physics-informed**)

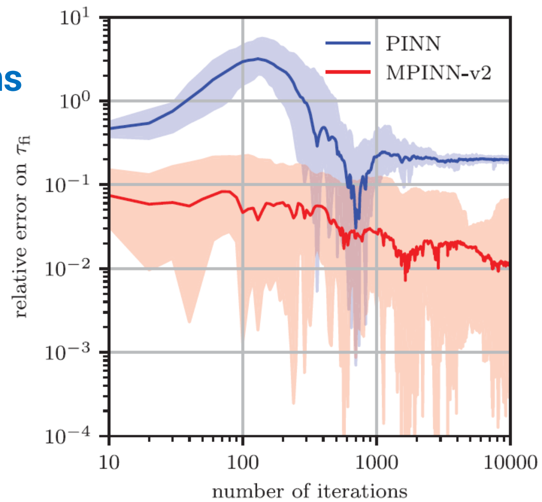

F. Regazzoni, S. Pagani, A. Cosenza, et al., *Rendiconti Lincei Matematica e Applicazioni*, 2021

Physics-driven meet AI algorithms

A data-driven emulator of cardiac chambers

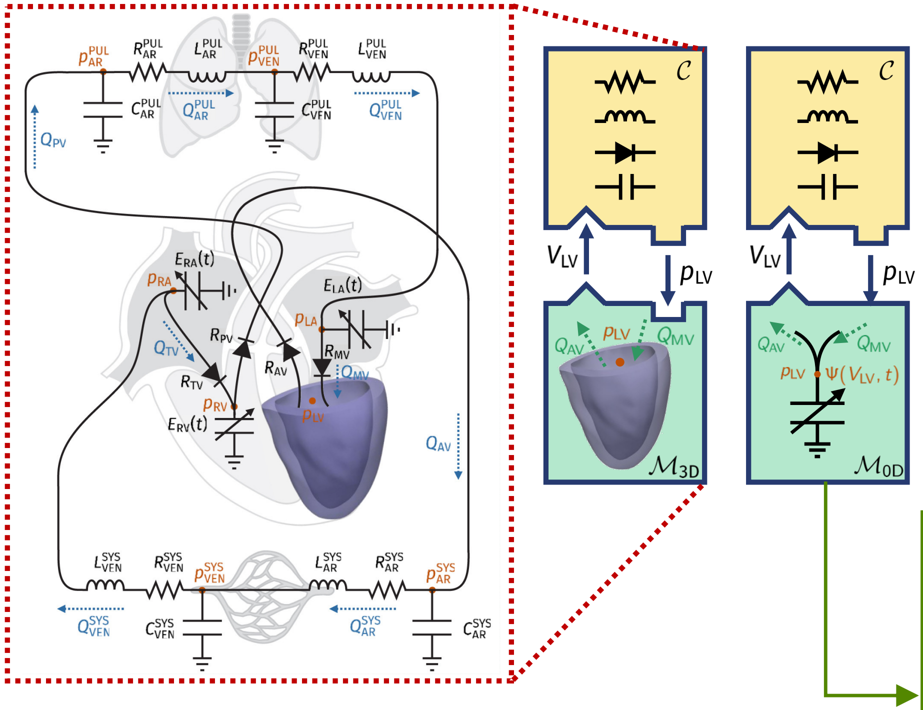

Method: we construct an emulator of the time-dependent pressure-volume relationship of each cardiac chamber, fitted from a few cycles obtained with the 3D-0D model

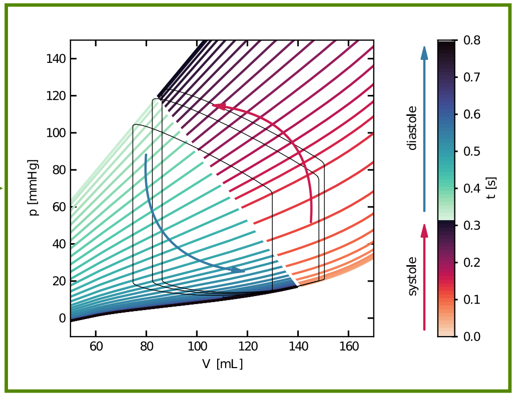

Challenge: the numerical cost of cardiac EM models is very large, and several cycles are needed to reach the limit cycle

V-cycle (3D-0D-3D)

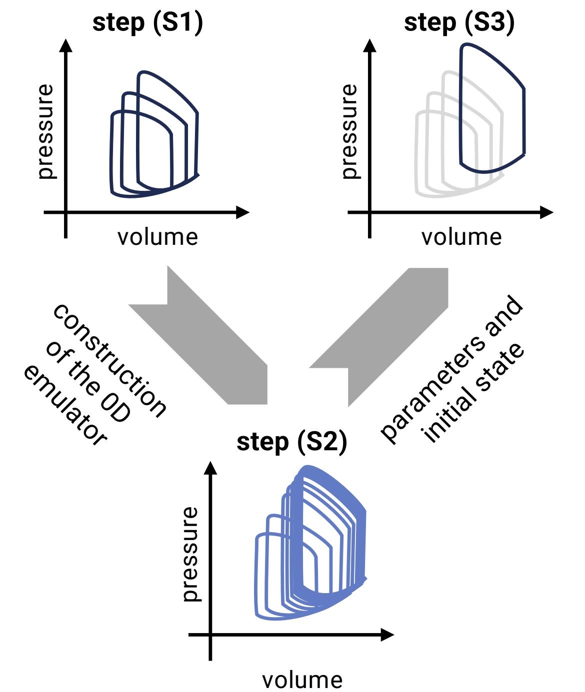

Parameter calibration and convergence to the limit cycle is done using a fully 0D model

F. Regazzoni, A. Q., *Computers in Biology and Medicine*, 2021

ANN-based surrogate of the LV electromechanical function

By means of **model-learning**, we construct a surrogate model of the LV electromechanical function, accounting for the dependence on **parameters.**

The model is trained from a set of 40 simulations obtained by sampling the parameter space.

The testing accuracy is remarkably good (relative error lower than 0.01)

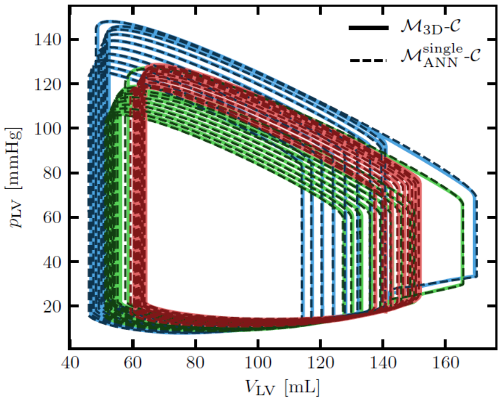

The surrogate model is reliable also for longer time-horizons than those considered in the training set!

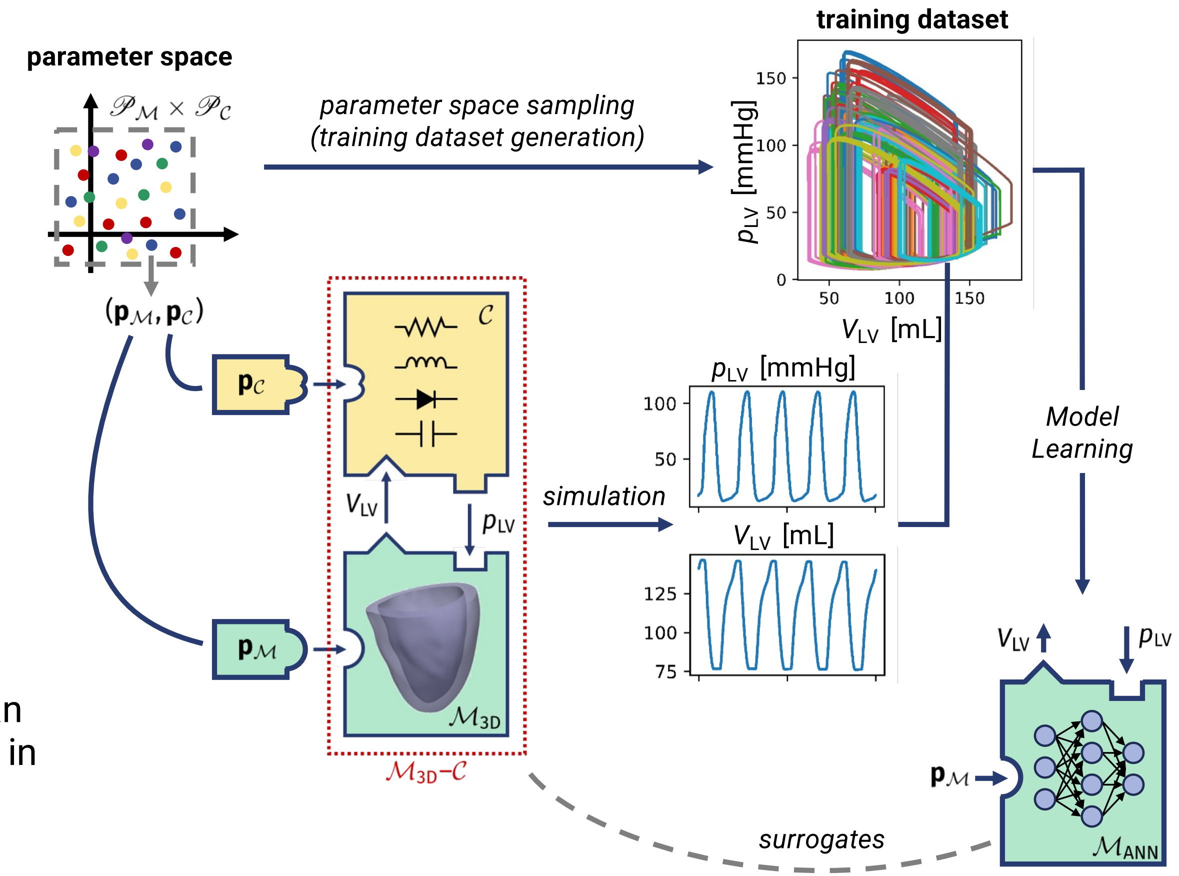

F. Regazzoni, L. Dede', A. Q., *Journal of Computational Physics*, 2019
F. Regazzoni, M. Salvador, L. Dede', A. Q., *Computer Methods in Applied Mechanics and Engineering*, 2022

ANN-based surrogate model for global sensitivity analysis

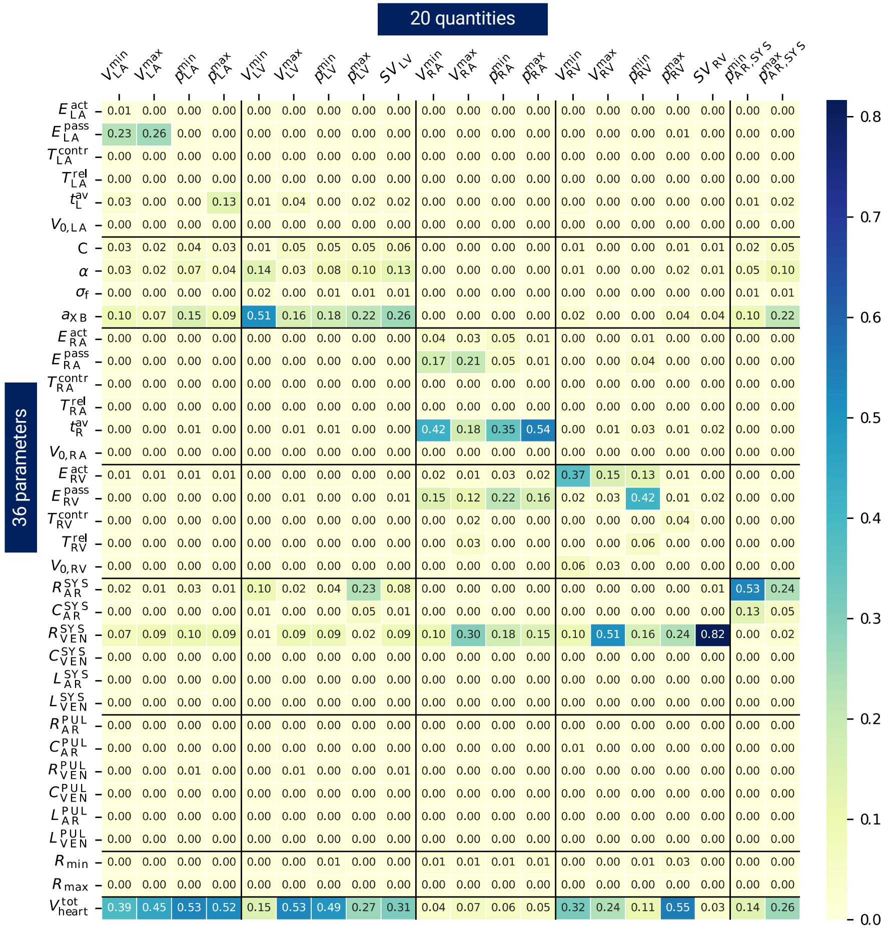

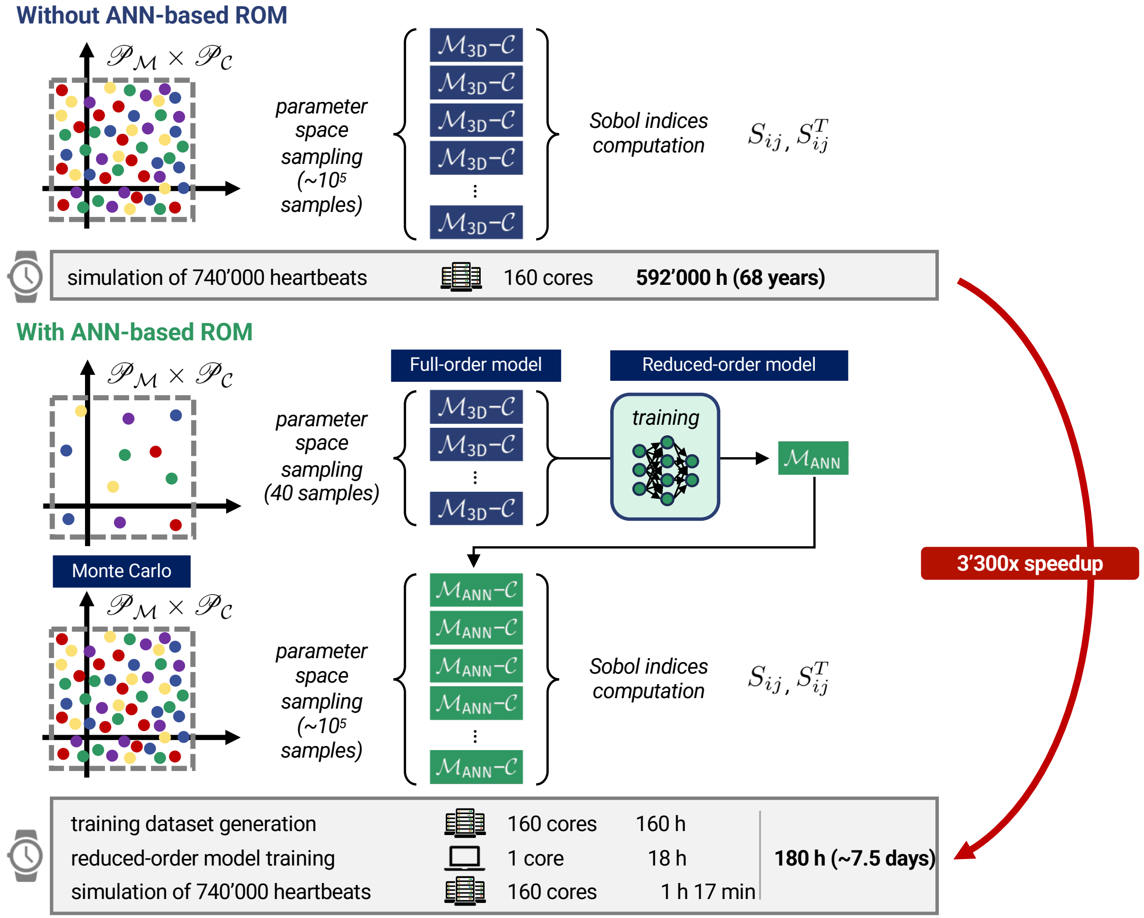

F. Regazzoni, L. Dede', A. Q., *Journal of Computational Physics*, 2019
F. Regazzoni, M. Salvador, L. Dede', A. Q., *Computer Methods in Applied Mechanics and Engineering*, 2022

ANN-based surrogate model for Bayesian parameter estimation

$\mathcal{F}: \mathbf{p} \mapsto \mathbf{q}$ Parameters-to-QoIs map

$\mathbf{q}_{\text{obs}} = \mathcal{F}(\mathbf{p}) + \epsilon \qquad \epsilon \sim \mathcal{N}(\cdot|\mathbf{0}, \Sigma)$ Σ = noise covariance

$\pi_{\text{prior}}(\mathbf{p})$ Prior distribution (prior knowledge on the parameters)

Posterior distribution (evaluated through Monte Carlo Markov Chain):

$$\pi_{\text{post}}(\mathbf{p}) = \frac{1}{Z} \mathcal{N}(\mathbf{q}_{\text{obs}}|\mathcal{F}(\mathbf{p}), \Sigma)\, \pi_{\text{prior}}(\mathbf{p})$$

Test Case:

Observed QoIs:
- Maximum arterial pressures
- Minimum arterial pressures

Unknown parameters:
- Myocardial contractility
- Systemic arterial resistance

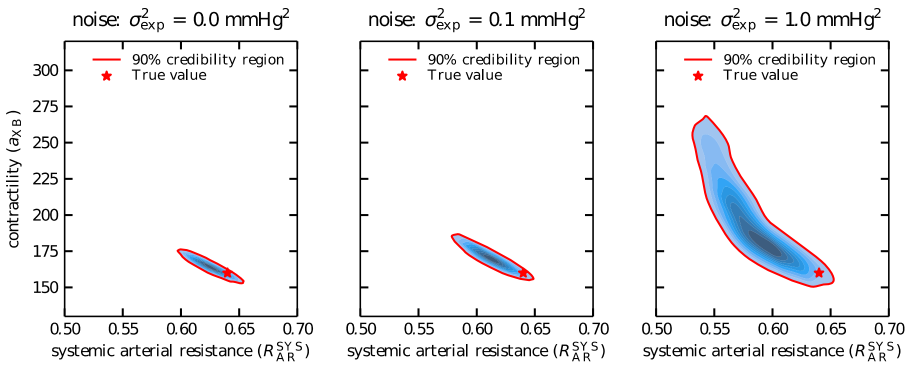

Without ANN-based ROM

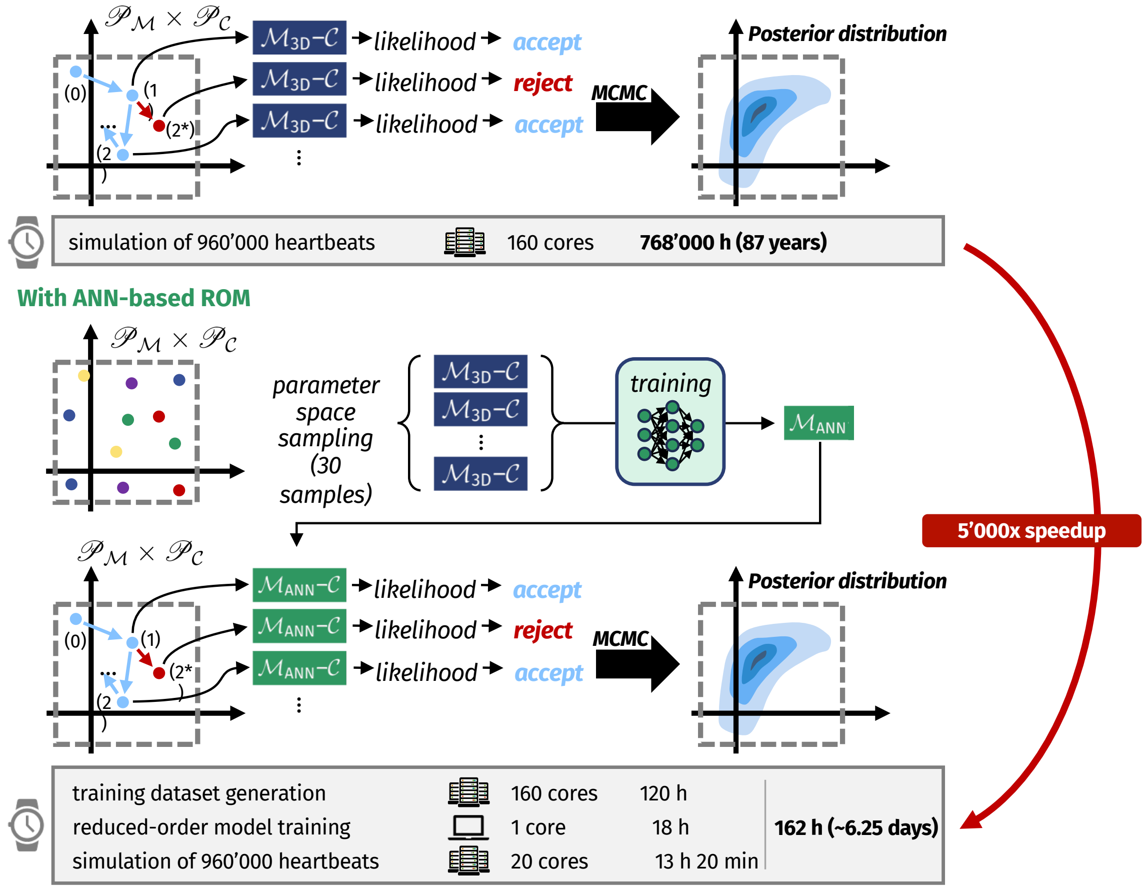

F. Regazzoni, L. Dede', A. Q., *Journal of Computational Physics*, 2019
F. Regazzoni, M. Salvador, L. Dede', A. Q., *Computer Methods in Applied Mechanics and Engineering*, 2022

DL-enhanced physics-based ROMs for cardiac mechanics

Full order: finite element method
- high fidelity ✓
- many degrees of freedom ✗
- computationally demanding ✗

Galerkin ROM: projection on linear space
- physics-based ✓
- few degrees of freedom ✓
- still depends on high-fidelity dimension ✗

Deep-HyROMnet: Galerkin-ROM with ANN approximation of non-linear operators
- physics-based ✓
- few degrees of freedom ✓
- independent of high-fidelity dimension ✓

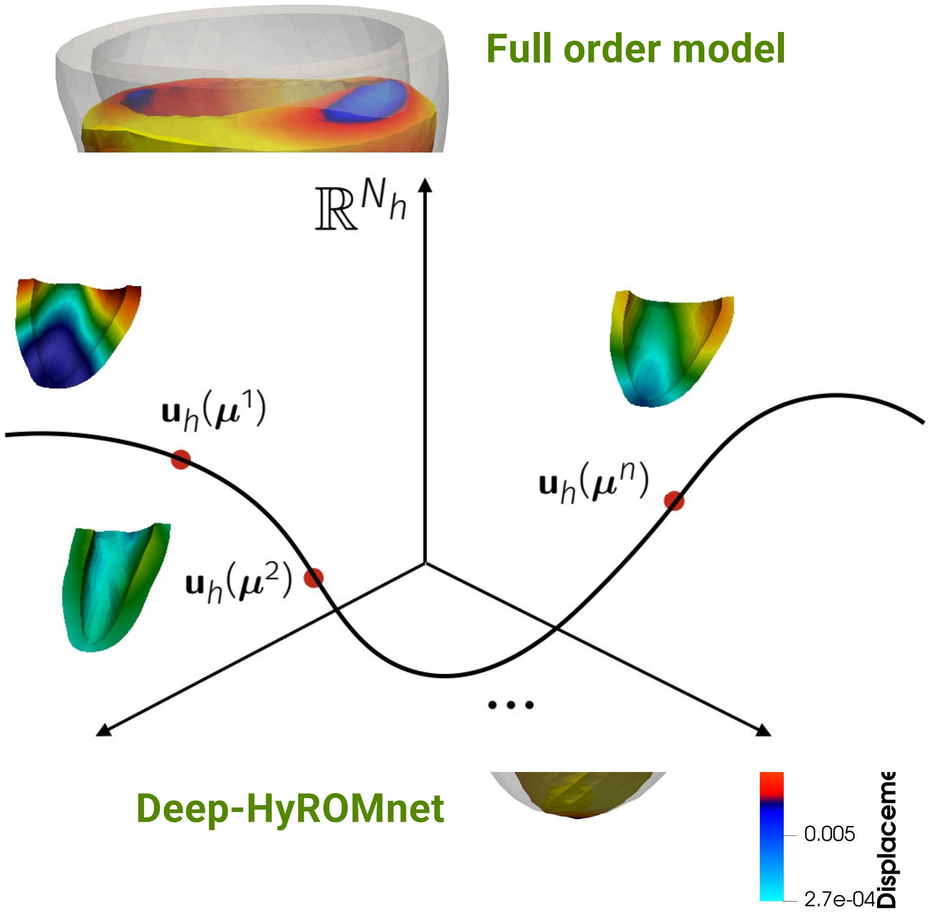

L. Cicci, S. Fresca, S. Pagani et al., *Mathematics in Engineering*, 2022
L. Cicci, S. Fresca, A. Manzoni, *Journal of Scientific Computing*, 2022 (accepted)

Physics-aware NN for inverse problems in electrophysiology

Goal: reconstruct the ventricles electrical activity from non-invasive recordings of the body surface potential (inverse problem of electrocardiography)

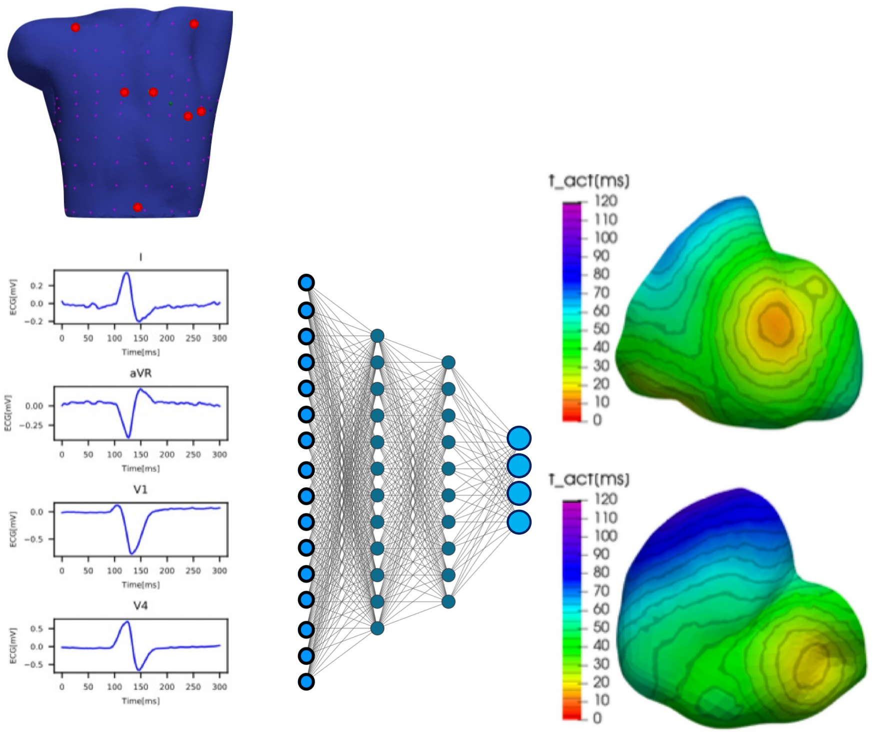

Method: train a physics-aware Neural Network (autoencoder) characterized by:

- Physical awareness (I): a projection based reduced-order model efficiently encodes the "forward map"
- Generalization: model performs well also in small data regimes.

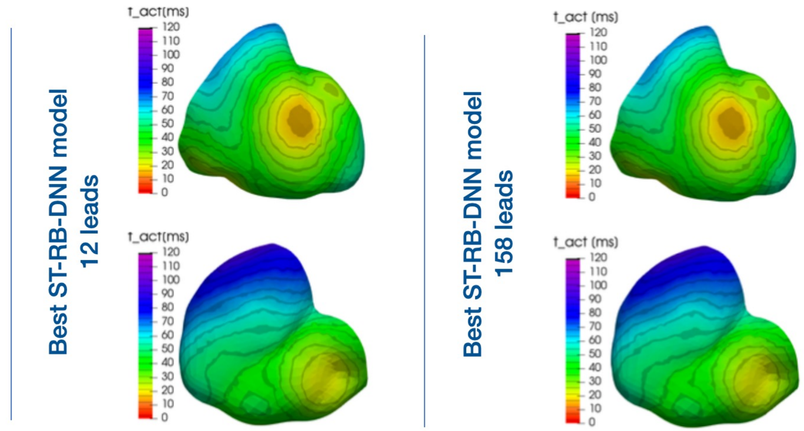

Results: the physics-aware NNs reconstruct activation maps with a 4% mean relative error, requiring only 10 minutes training on a regular laptop

R. Tenderini, S. Pagani, S. Deparis, A. Q., *SIAM Journal on Scientific Computing*, 2022

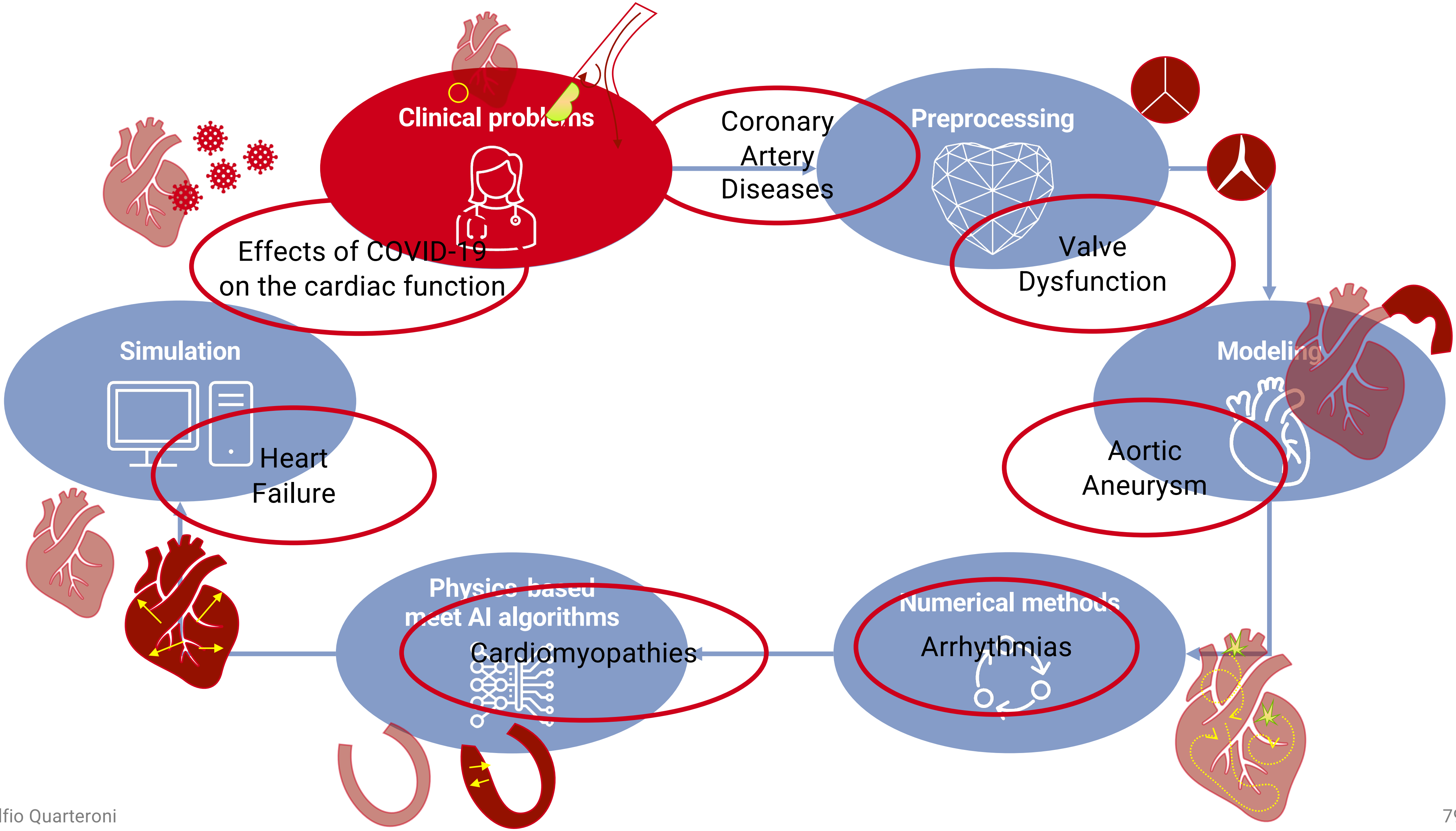
Clinical problems
Coronary Artery Diseases
Preprocessing
Valve Dysfunction
Modeling
Aortic Aneurysm
Numerical methods
Arrhythmias
Physics-based meet AI algorithms
Cardiomyopathies
Simulation
Heart Failure
Effects of COVID-19 on the cardiac function

Atrial fibrillation (AF)

Clinical question: which are the mechanisms behind AF progression?

IRCCS HUMANITAS RESEARCH HOSPITAL

I.R.C.C.S. Ospedale San Raffaele

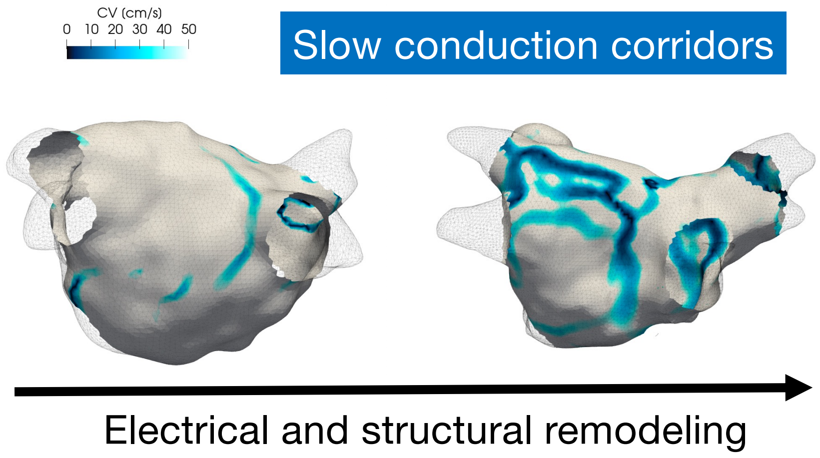

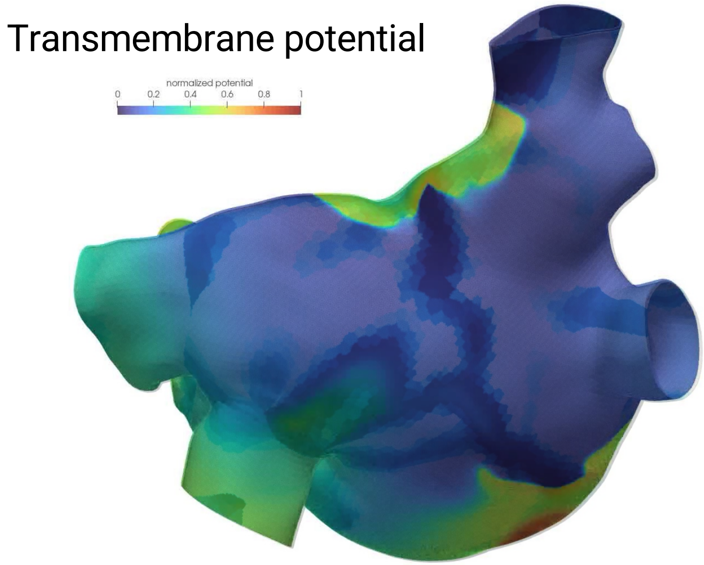

- **slow conduction corridors** and **pivot points** quantitatively characterize **AF progression**
- Numerical simulations confirm the role of **slow conduction corridors** in **AF sustainment** (localized reentry anchoring)

A. Frontera, S. Pagani, L.R. Limite et al., *JACC: Clinical Electrophysiology*, 2022
S. Pagani, L. Dede', A. Frontera et al., *Frontiers in Physiology*, 2021

Ventricular tachycardia

Simulation

Clinical question: which are the characteristics of VT circuits?

I.R.C.C.S. Ospedale San Raffaele

ventricular tachycardia

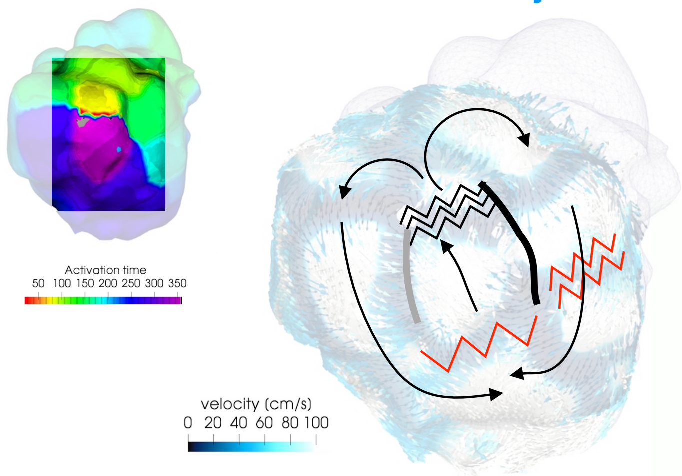

Functional line of block

Structural line of block

Functional slow conduction

Structural slow conduction

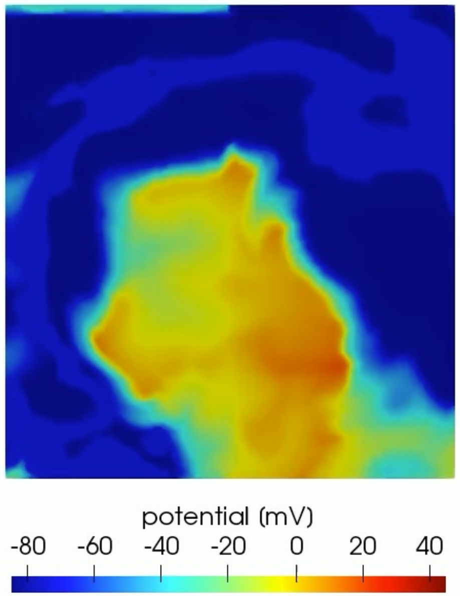

sinus rhythm

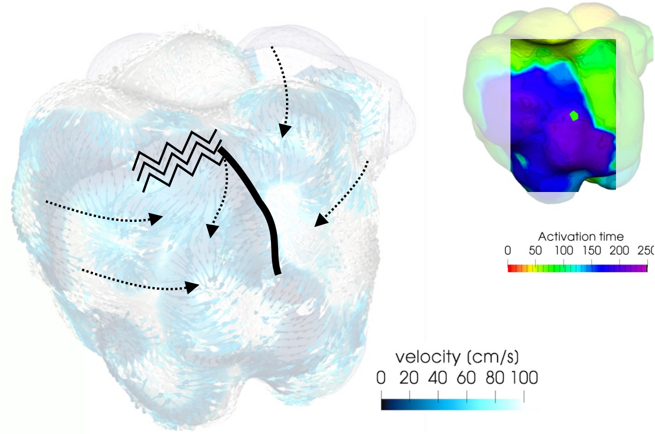

VT circuits contain both **functional** and **structural phenomena**

Functional phenomena not visible in sinus rhythm **can be predicted** by **numerical simulations**

A. Frontera, S. Pagani, et al, Heart Rhythm, 2020

Ventricular tachycardia and fibrillation

Clinical question: are ventricular tachycardia and fibrillation better simulated by accounting for mechanical deformation?

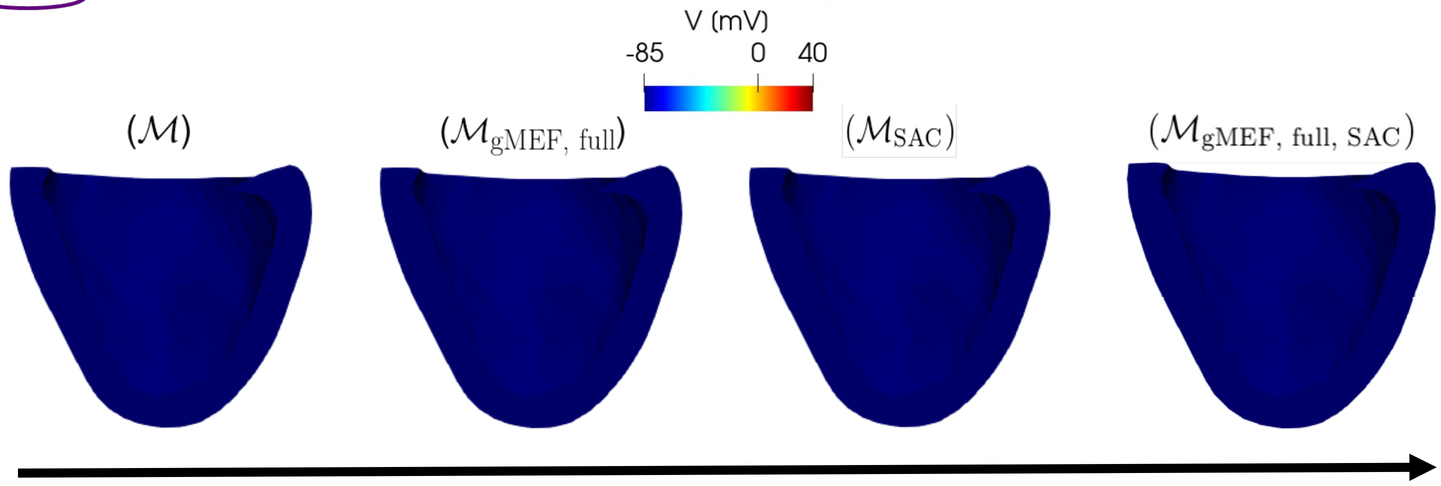

From **electrophysiology** to **electromechanics**
(**geometry-mediated mechano-electric feedbacks** and **stretch-activated channels**)

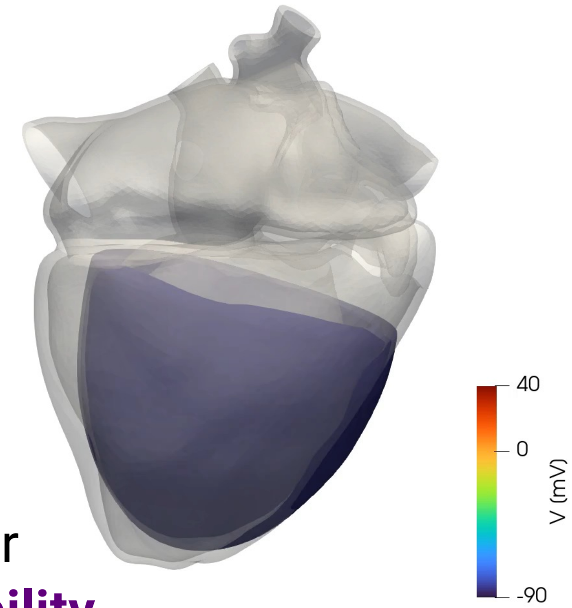

Electrophysiology and **electromechanics** simulations may differ in **conduction velocity**, **electric stability** and **hemodynamic stability**

M. Salvador, M. Fedele, P.C. Africa et al., *Computers in Biology and Medicine*, 2021
M. Salvador, F. Regazzoni, S. Pagani et al., *Computers in Biology and Medicine*, 2022

Simulation

Hypertrophic Cardiomyopathy (HCM)

Clinical question: can CFD simulations guide obstruction assessment and pre-operative design of septal myectomy?

Ospedale Luigi Sacco
AZIENDA OSPEDALIERA - POLO UNIVERSITARIO

SISTEMA SANITARIO REGIONALE
AZIENDA OSPEDALIERA SAN CAMILLO FORLANINI

non-obstructive HCM **obstructive HCM**

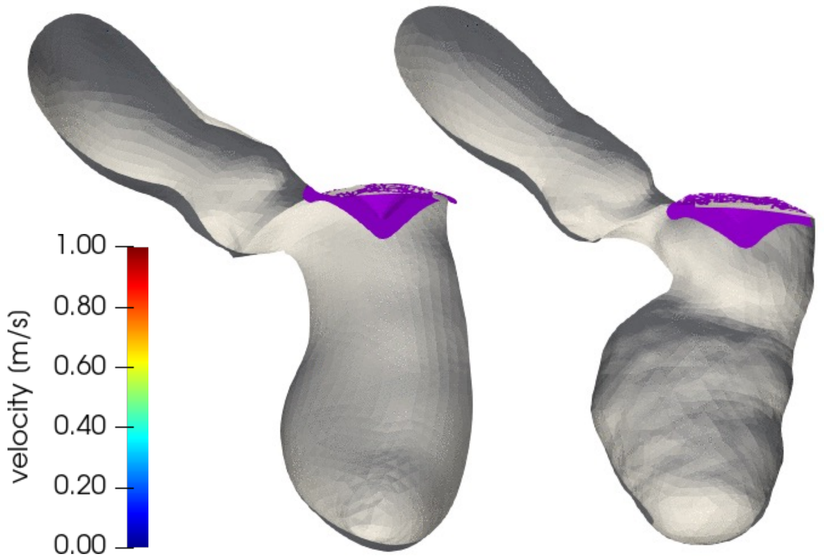

Obstructive HCM-induced **Venturi effect** causing systolic anterior motion

pressure along septum at systolic peak from coronary ostium down to the apex

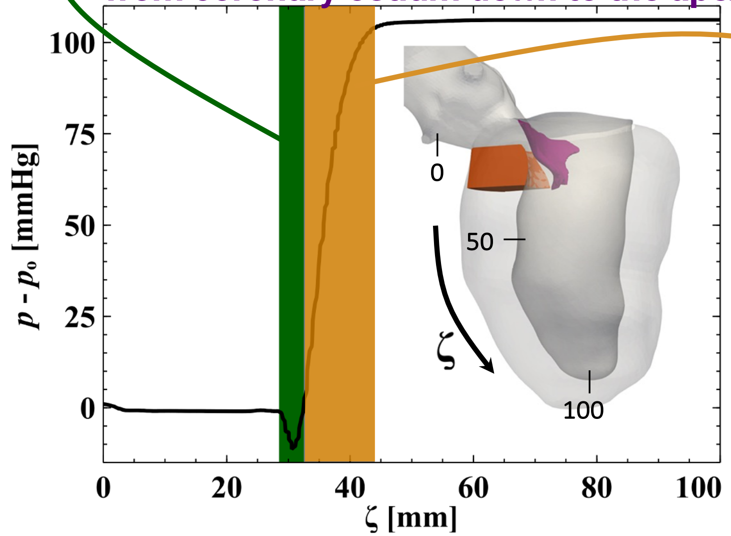

obstruction severity: **extent** and **amplitude** of **subaortic pressure gradient**

indication for surgical treatment: **portion to remove** by septal myectomy

I. Fumagalli, M. Fedele, C. Vergara, et al., *Computers in Biology and Medicine*, 2020
I. Fumagalli, P. Vitullo, C. Vergara, et al., *Frontiers in Physiology* , 2022

Transcatheter Aortic Valve Implantation (TAVI)

Clinical question: which are the predictive indicators of TAVI Structural Valve Deterioration (SVD)?

Centro Cardiologico Monzino

WSS at systolic peak

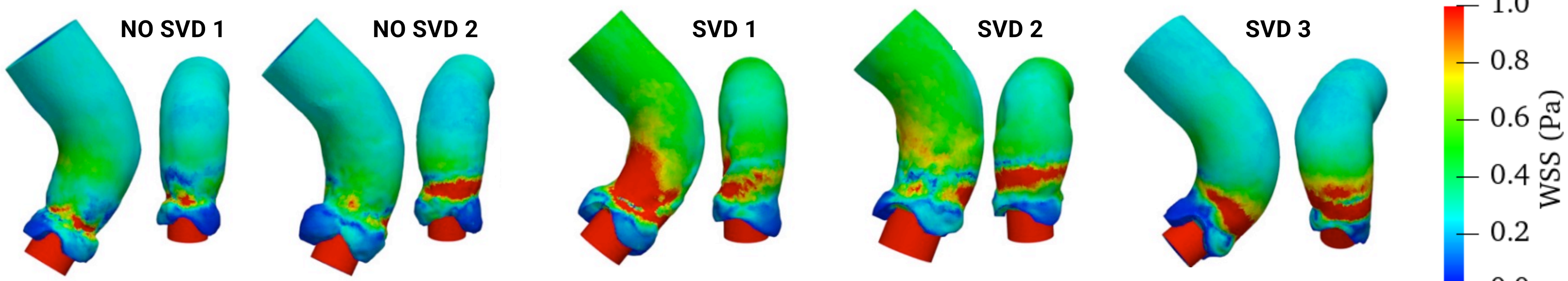

η = 1.34 % η = 1.31 % η = 5.84 % η = 3.50 % η = 13.95 %

- Analysis based on **pre-implantation** data only
- **WSS stronger** and more **persistent** in **SVD** cases
- ***η* index** discriminating SVD from NO-SVD, based on **Time-Averaged WSS (TAWSS) Critical Area (CA)**:

$$\eta = \frac{|CA|}{|\Gamma_{\mathrm{wall}}|}, \text{ with } CA = \{\mathbf{x} \in \Gamma_{\mathrm{wall}} : TAWSS(\mathbf{x}) > 0.5\mathrm{Pa}\}$$

I. Fumagalli, R. Polidori, F. Renzi et al., *MOX Report,* Politecnico di Milano, 2022

Estimating cardiac blood flow maps

Clinical question: can we replace CT scans and stress protocols with a computational estimation of myocardial blood flow maps?

Centro Cardiologico Monzino

Clinical pipeline

Adenosine injection → Stress-CTP scan → MBF maps

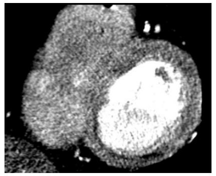

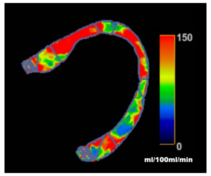

Consistency tests: calibration of **perfusion model** on available maps yields **excellent agreement**

Ongoing: calibration of patient-specific models based on **pressure data only** (no maps)

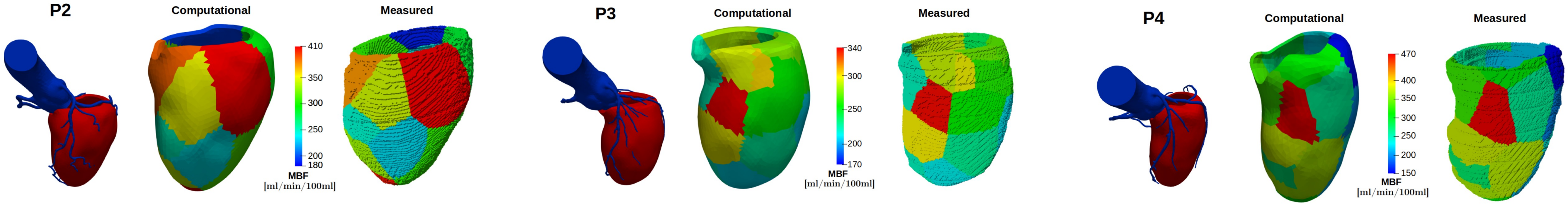

S. Di Gregorio, C. Vergara, G. Montino Pelagi et al., *European Journal of Nuclear Medicine and Molecular Imaging* 2022

Simulation

Transcatheter Aortic Valve Implantation (TAVI)

Clinical question: predict long-term durability of the implanted bio-prosthetic valve

Centro Cardiologico Monzino

Group of Dr. G. Pontone

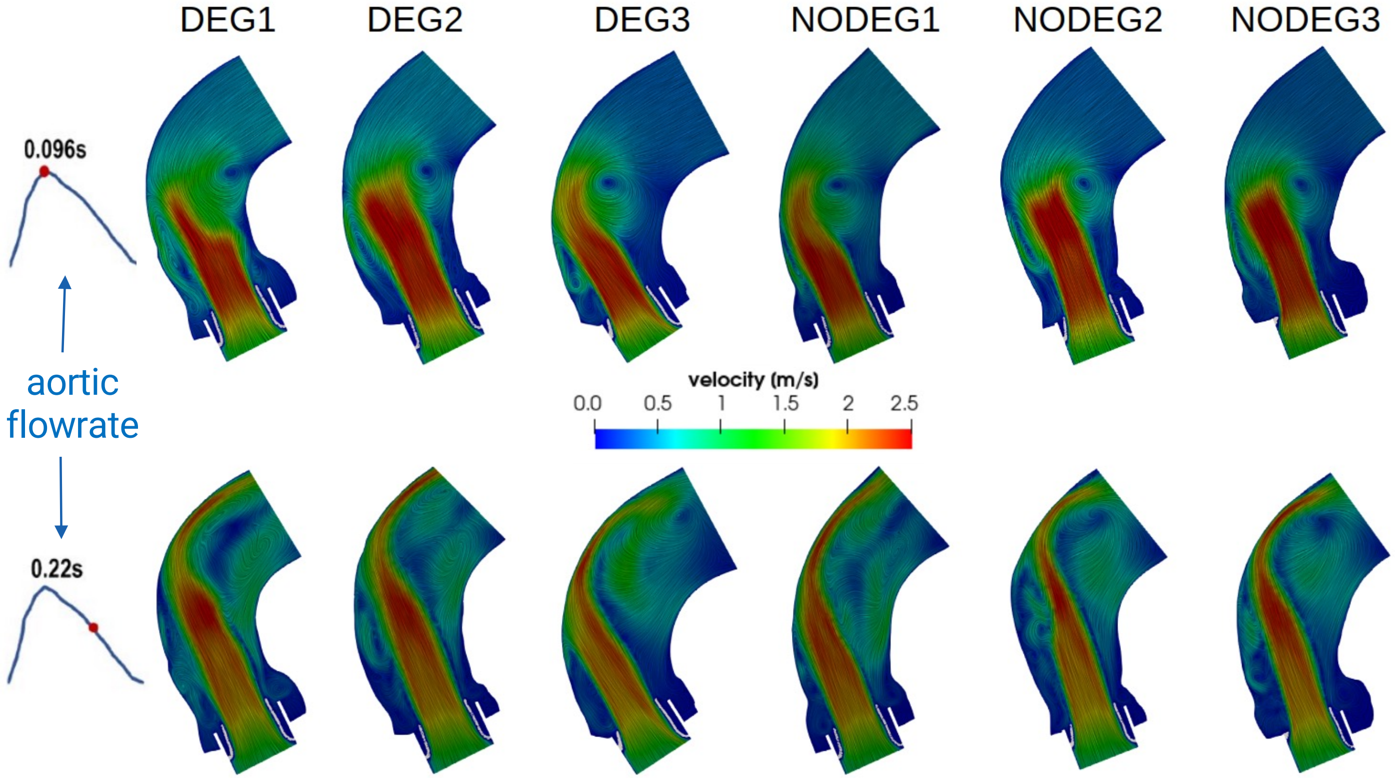

Study population

6 patients with **follow-up**:

3 degenerated valves

3 non-degenerated valves

Blood velocity field in presence of TAVI valve

Simulation

I. Fumagalli, R. Polidori, F. Renzi et al., *Int J Num Meth Biomed Eng, 2023*

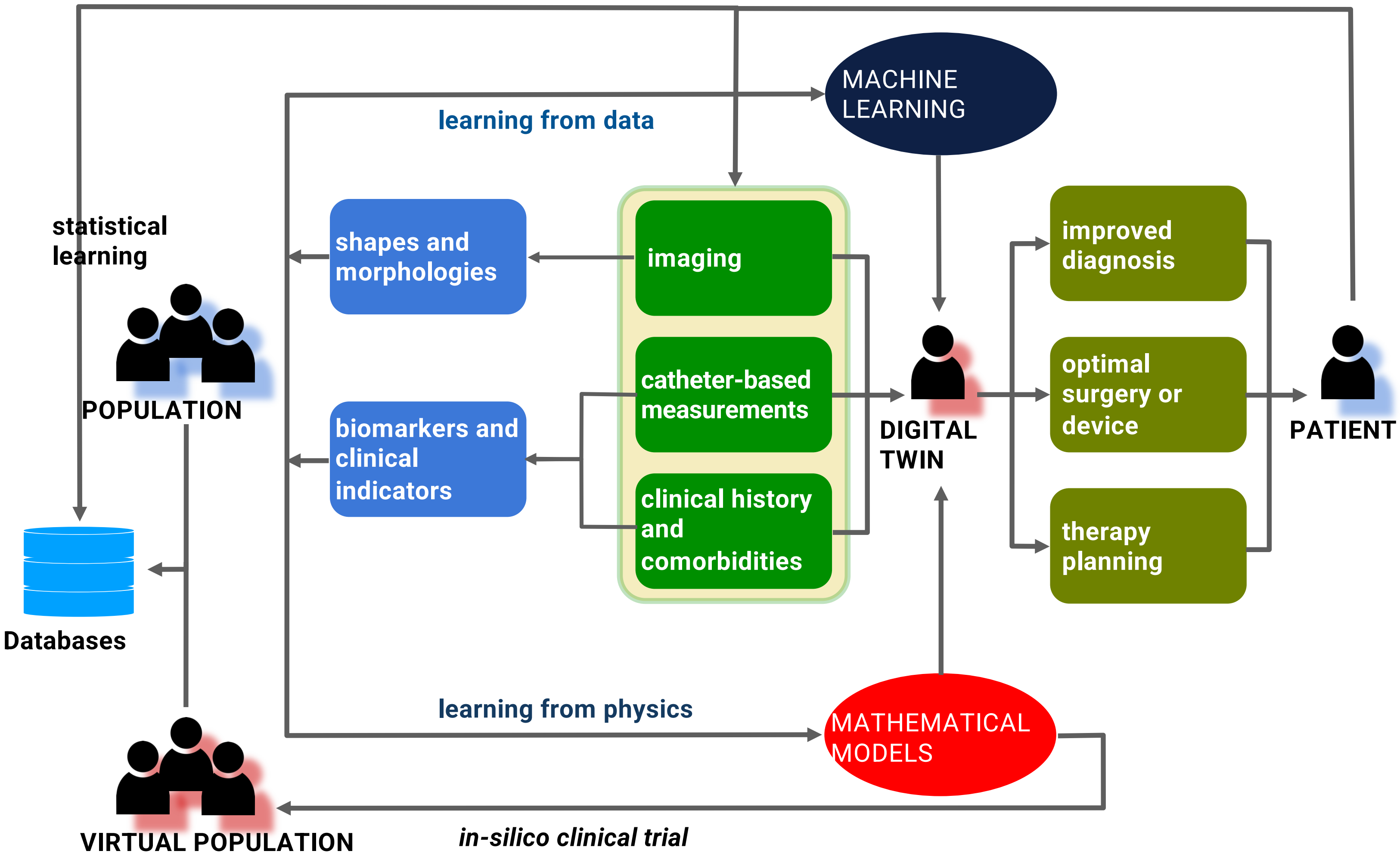

MACHINE LEARNING
learning from data
statistical learning
shapes and morphologies
imaging
POPULATION
catheter-based measurements
biomarkers and clinical indicators
clinical history and comorbidities
DIGITAL TWIN
improved diagnosis
optimal surgery or device
therapy planning
PATIENT
Databases
learning from physics
MATHEMATICAL MODELS
VIRTUAL POPULATION
in-silico clinical trial

THANK YOU
from
The iHEART simulator
team